Studies of Basin Heat Balance and Snowmelt Runoff Models*

by

Hideaki MOTOYAMA
本 山 秀 明
The Institute of Low Temperature Science

Received December 1986

Abstract

Snowmelt and snowmelt runoff were observed hydrologically and meteorologically in winter and snowmelt season at a watershed, 11.2 km^2 in area, in the northern part of Hokkaido, Japan. On the basis of the observations the water balance of the watershed in these seasons were studied and models were developed for the snowmelt runoff.

The amount of snowmelt at snow-ground interface (bottom-melt) was measured continuously by the lysimeter in two winters at the outlet of the basin constituting the watershed. The value obtained agreed well with the amount of bottom-melt estimated from a heat balance at the snow-ground interface. The amount of bottom-melt was found dependent mainly upon air temperature and snow depth. Then, the amount of bottom-melt in the entire watershed was estimated using air temperatures and snow depths. A comparison between this estimate and the observed amount of runoff of the watershed revealed that the bottom-melt supplied about one half of the amount of runoff. Meanwhile, a runoff tank model was developed; it gave a good simulation of the observed amount of runoff.

The surface snowmelt distributions in the watershed and the amount of snowmelt runoff in three snowmelt seasons were observed and the water balances were examined. It was further found that 90 % of the snow covering the watershed runs off as stream flow.

The heat balance method was applied for the entire watershed in order to estimate the snowmelt distribution. The hourly total snowmelt was compared with the runoff, and a runoff tank model, which takes into account percolation through the snowpack, was obtained. It simulated well the hourly runoff of the watershed.

* Contribution No. 2930 from the Institute of Low Temperature Science.
北海道大学審査学位論文

Contents

I. Introduction

I.1 *Introduction*

Most areas of Japan are covered with deep snow for six months or more of the year. In these areas the accumulated snow constitutes one of the main water resources for much of the year, and the amount of snow has a strong effect on the characteristics of the runoff. However, this effect has not been fully understood. The winter runoff cultivated partially by melting at the snow-ground interface has been ignored by many hydrologists because it makes only a small contribution to the annual discharge of the watershed and it is difficult to measure hydrological components including the flow rate of the snow-covered river and the rate of melting at the snow-ground interface.

Investigators have primarily studied the forecasting of the amount of runoff in snowmelt season (defined as the period during which snow melts at the surface everyday) and have proposed several methods and models for runoff forecasting. However, almost all of these methods and models were to estimate the daily amount of runoff. In order to forecast a flood resulting from a sudden increase in the amount of runoff, a model is necessary for estimating the hourly amount (or for a shorter interval) of runoff.

This study attempted to develop a model for this forecasting. Based on the observed amounts of snowmelt (at the surface and the bottom of the snowcover) and meteorological elements at a station, a discussion was made of a method used for estimating the amount of snowmelt from a heat balance. Then this method was extended to obtain the amount of snowmelt in the entire watershed. Using the amount obtained, the water balance was studied and a model was developed for forecasting the runoff, drawing on Sugawara's tank model (Sugawara et al., 1984). The recession rate of a runoff hydrograph, which indicates the characteristics of the runoff response of the watershed, was used to determine the structures and the coefficients of the runoff tank model. This runoff model indicated the physical process of runoff, even though it is a black box model.

Following this introduction, the study area will be described and in the end of this chapter the heat balance model for the snowcover, which is used to obtain the amount of snowmelt, will be briefly explained. In Chapter II, the effect of melting at the snow-ground interface on the runoff in winter will be described. The study of snowmelt runoff in snowmelt season will be described in Chapters III and IV, in which Chapter III will be devoted to a discussing of the water balance based on hydrological observations in three seasons, introducing a model developed for obtaining the daily amount of runoff. For the purpose of forecasting a flood resulting from the runoff, the amount of snowmelt in the entire watershed will be calculated by the heat balance method, and a model will be developed for obtaining an hourly runoff. These procedures will be explained in Chapter IV. Finally

concluding remarks will be given in Chapter V.

I.2 *Study area*

Observations were carried out at an experimental watershed located in the northern part of Hokkaido, Japan, at 44°23′N, 142°17′E. The area of the watershed is 11.2 km². The elevation ranges from 280 m to 630 m a.s.l. (Fig.1a). Slope directions are shown in Fig. 1b. The south and the west slope areas are slightly larger than the other areas. The average inclination of the entire watershed is 11.0°. The forest is sparse and mixed,

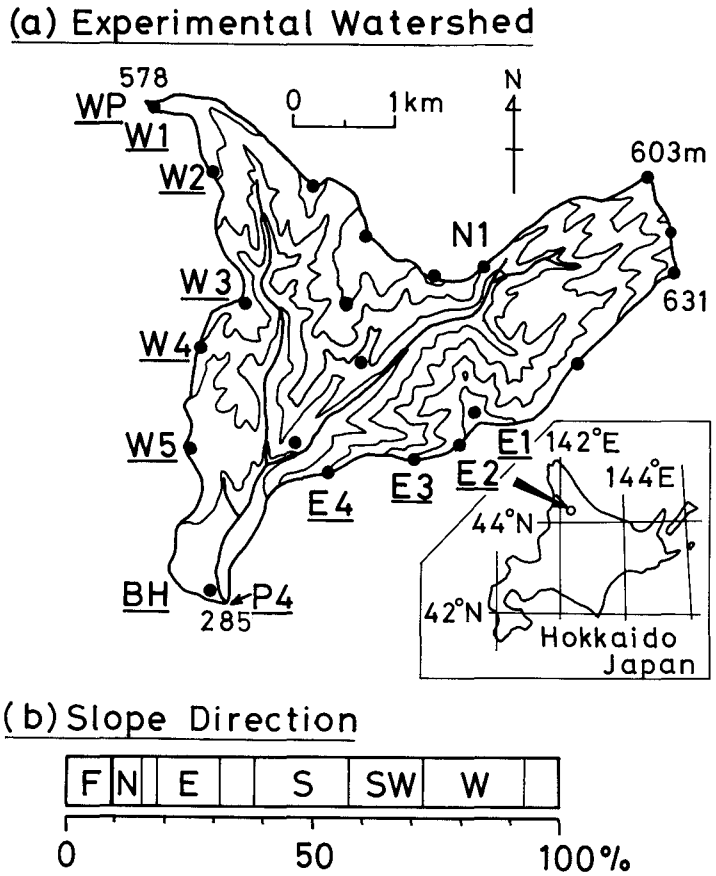

Fig. 1 (a) Location map of the experimental watershed. Solid circles indicate the points where measurements are made of snow water equivalents and snow melting rates. BH and WP stations are for meteorological observations. P4 point is for water gauge station. (b) The distribution of slope directions. The slopes are broken down into eight directions and a flat area.

composed of broad-leaved trees (80%) and coniferous trees (20%).

This area is well known in Japan as one of the areas lowest in air temperature and deepest in snow accumulation. The lower region of the watershed is covered with snow for about seven months of the year with the snow depth usually reaching 2.0 – 2.5 m. In mid-winter, the air temperature sometimes falls to below −40°C. Snow seldom melts at the snow surface in winter. The snowmelt season starts in early April, and the snowcover disappears by mid-May. Details of the hydrological and meteorological characteristics of the watershed were described by Kojima et al. (1970, 1971) and Kobayashi and Uematsu (1977).

I.3 *Heat balance of snowcover*

The amount of snowmelt can be estimated by studying the components of a heat balance. Discussed in this section is the heat balance for the snowcover.

The heat balance of the entire snow layer is dealt with an assumption that horizontal heat fluxes are absent. Let the sign of heat received by the snowcover be positive. The heat balance equation of the snowcover is then written as (Fig. 2),

$$\begin{aligned} QM &= QU + QB \\ &= (QR + QA + QE - QC + Qr) \\ &\quad + (Q_{cg} - Q_{cs}), \end{aligned} \tag{1}$$

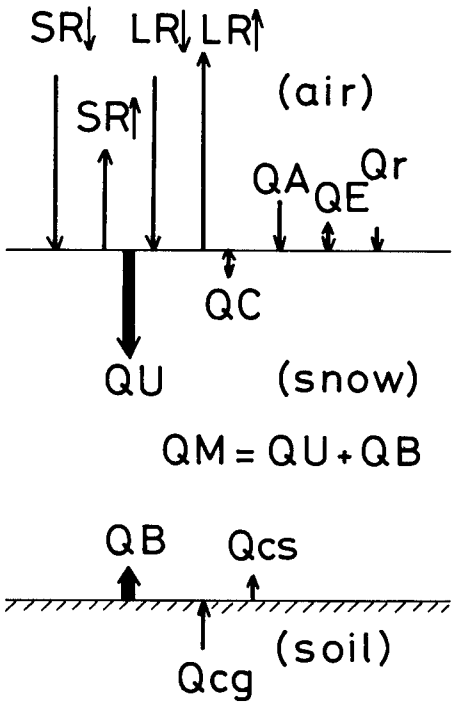

Fig. 2 Heat balance of snowcover. $QR = SR\downarrow - SR\uparrow + LR\downarrow - LR\uparrow$. The details are described in the text.

where QM is the energy flux available for snowmelt; QU and QB are the fluxes of heat at the snow-air and the snow-ground interface, respectively; they are divided to five and two components as follows: As for QU, QR: net radiation; QA: sensible heat flux from the air; QE: latent heat flux; QC: conductive heat flux through the snowcover; and Qr: flux of heat from rain. And as for QB, Q_{cg}: conductive heat flux in the ground; and Q_{cs}: conductive heat flux in the snow.

In the winter season, snow seldom melts at the surface in this watershed ($QU = 0$); so, Equation (1) can be rewritten as,

$$QM = QB = Q_{cg} - Q_{cs}. \tag{2}$$

In the snowmelt season, on the other hand, the amount of surface melt is ten times or more greater than the amount of bottom-melt ($QU \gg QB$); so Equation (1) can be written as,

$$QM = QU = QR + QA + QE - QC + Qr. \tag{3}$$

Equations (2) and (3) are used for estimating the amount of snowmelt in the watershed.

II. Snowmelt runoff in winter

II. 1 *Introduction*

The specific runoff from a watershed (the rate of discharge divided by the drainage area, $m^3s^{-1}km^{-2}$) in snowy regions is, in general, greater than that in snow-free regions (Arai; 1976, 1980). However, the cause of this phenomenon has not been studied quantitatively. Recently, Kojima and Motoyama (1985) and Motoyama et al. (1986a) reported that in a region with deep snow the conductive heat flux from the ground caused snow to melt continuously at the bottom of snowcover and the bottom-melt influenced the storage of groundwater, with the resultant increase in the amount of runoff of the stream in winter. Although the amount of runoff is much smaller in winter than that in snowmelt season, it is necessary to develop a model for winter runoff, which takes into account the effect of the bottom-melt of the watershed. This type of model will contribute to better control of water resources in winter.

The purposes of this part of the study are : (1) to establish a method for calculating the amount of bottom-melt using meteorological and hydrological data at a station ; (2) to extend the method established to the entire watershed and compare its result with the observed amount of runoff ; (3) to develop a model for winter runoff on the basis of the result of (2).

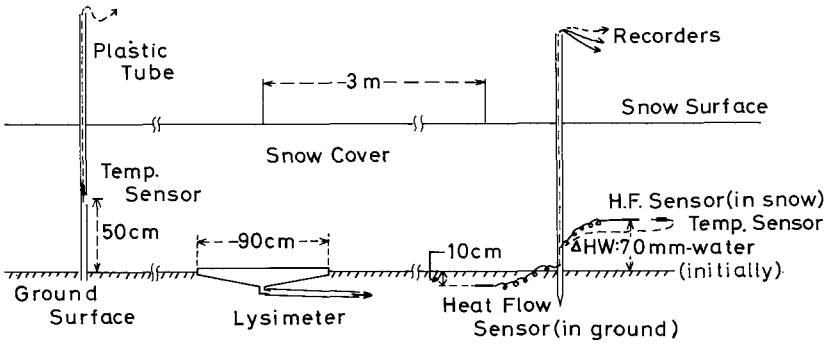

Fig. 3 The schematic diagram of installation of the lysimeter, heat flow sensors, and temperature sensors at BH station.

II. 2 *Instrumentation*

The meteorological and hydrological observations were carried out at BH station in the watershed (Fig. 1). The observed periods were from December to March in 1981−82 and 1983−84. The objects observed and the instruments used were: (1) The amount of snowmelt at the snow-ground interface (bottom-melt) was observed continuously by a shallow lysimeter, 0.9×0.9 m^2 in area and 0.1 m in depth at its center. It was installed on top of the level ground (Fig. 3). (2) Conductive heat fluxes in the ground and in the snowcover were continuously measured by heat flow sensors. (3) Air temperature and snow depth were continuously measured by platinum resistance thermometers and by snow stakes, respectively. (4) Snow water equivalents, snow temperature profiles, and snow density profiles were obtained from snow pit observations performed once or twice a month. (5) The discharge at the outlet of the watershed was obtained once or twice a month, measuring the vertical cross sectional area and the flow velocity of the river. The snow accumulation at the river shore and the ice formation at the river surface changed the vertical cross sectional area, making it impossible to apply the relationship between the water level and the discharge in the snow-free season for obtaining the discharge in the snowy season. Therefore, the water level continuously recorded by the water gauge was not used for the determination of the discharge.

In the 1983−84 winter season, time variations of snow depth were obtained automatically by snow depth recorders of the optical fiber type (Aburakawa, 1980) at five stations (BH, W1, N1, E1, E4, see Fig. 1).

II. 3 *Results of observations at BH station*

The air temperature, averaged for every five days, and the snow depth, are shown in Figs. 4 and 5, respectively. The mean air temperature and maximum snow depth from December to March were −9.0°C and 2.6 m in 1981−82, and −10.9°C and 1.8m in 1983−84. Therefore, there was heavy snow and high temperature in the 1981−82 winter relative to those in the 1983−84 winter.

The daily amount of bottom-melt, m_b, obtained by the lysimeter is shown in Fig. 6 (LY, solid line). In the 1981−82 winter with heavier snow, m_b decreases gradually from the maximum value of about 1.2 mmd^{-1} in early December, reaches the minimum value of 0.2−0.3 mmd^{-1} in February, and then increases again afterwards (Fig. 6a). In the 1983−84 winter (Fig. 6b) with less snow, however, m_b shows the same pattern as the above, but short-period fluctuations in the amount of m_b seen in both the winters seemed to depend on air temperature fluctuations. From these results it was deduced that the bottom-melt was dependent on the snow depth and the air temperature.

Figure 6 also shows the daily amount of runoff depth r (daily amount of discharge divided by the drainage area, mmd^{-1}), which decreases steadily from the value of 1.0−1.5 mmd^{-1} in

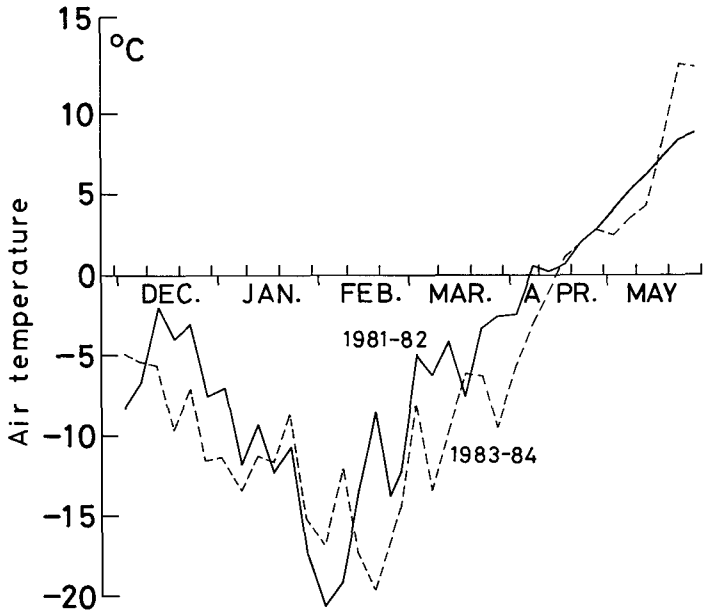

Fig. 4 Air temperature averaged for every 5 days at BH station. Solid line: 1981−82, broken line: 1983−84.

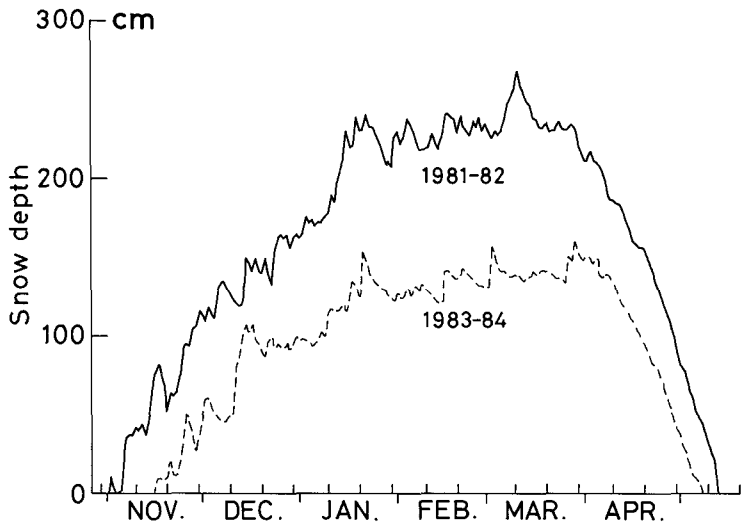

Fig. 5 Variation in snow depth with time at BH station. Solid line: 1981−82, broken line: 1983−84.

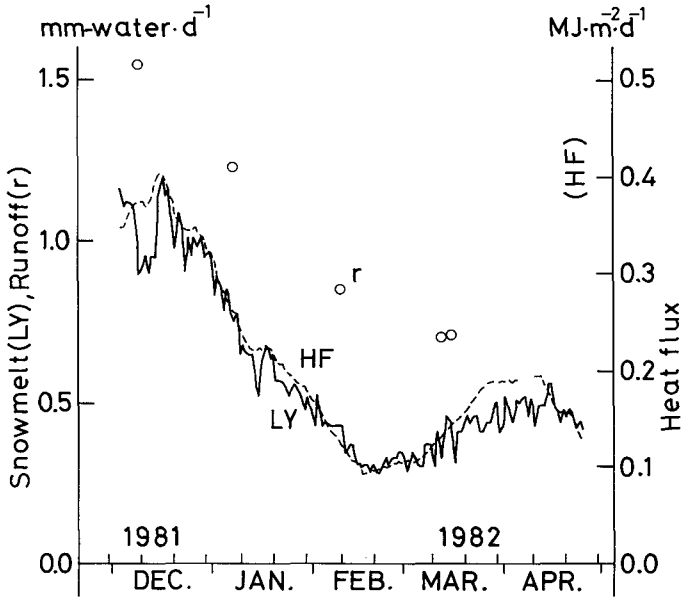

Fig. 6a Time variations in the amount of bottom-melt at BH station and the amount of runoff during the 1981−82 winter.
Solid line : daily amount of bottom-melt by the lysimeter (LY).
Broken line : amount of bottom-melt estimated by $(Q_{cg}-Q_{cs})/L_m$ (HF).
Open circles : daily amount of runoff depth (r).
Left ordinate represents the rate of snowmelt or runoff depth. Right ordinate represents the amount of energy for snowmelt.

December to the value of 0.6−0.7 mmd^{-1} in March. Both m_b and r were slightly larger in 1981−82 than those in 1983−84.

II. 4 *Method for calculating heat flux in snowcover*

The upward heat flux in the ground, Q_{cg}, is almost always larger than that in the snowcover, Q_{cs}. Figure 7 shows time variations in heat fluxes Q_{cg} and Q_{cs} in the 1981−82 winter (Fig. 7a) and in the 1983−84 winter (Fig. 7b). The heat balance equation at the snow-ground interface is rewritten as,

$$QM = QB = Q_{cg} - Q_{cs}. \tag{2}$$

The estimated amount of bottom-melt, m_b(HF), can then be given by,

$$m_b(\mathrm{HF}) = QM/L_m = (Q_{cg} - Q_{cs})/L_m, \tag{4}$$

where L_m is the latent heat of melting ice. Values of Q_{cg} and Q_{cs} were measured by the heat flow sensors, and m_b(HF) was calculated using Equation (4). The value of m_b(HF) (shown

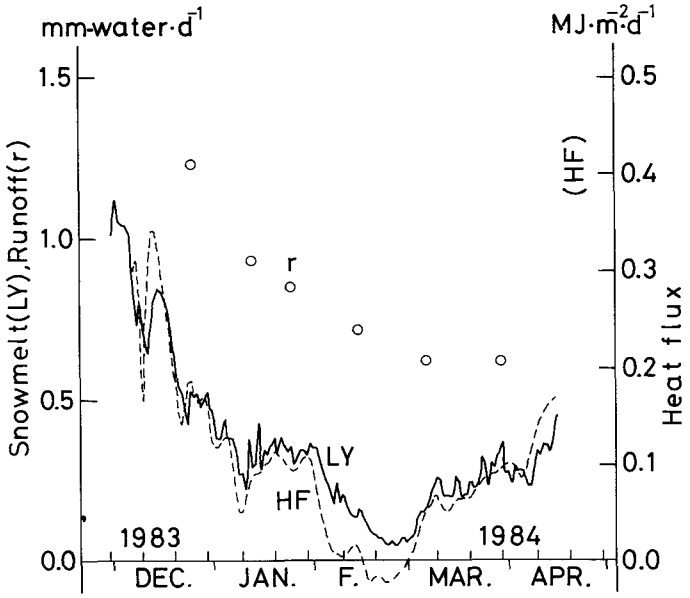

Fig. 6b Time variations in the amount of the bottom-melt at BH station and the amount of runoff during the 1983–84 winter. Notations are the same as in Fig. 6a.

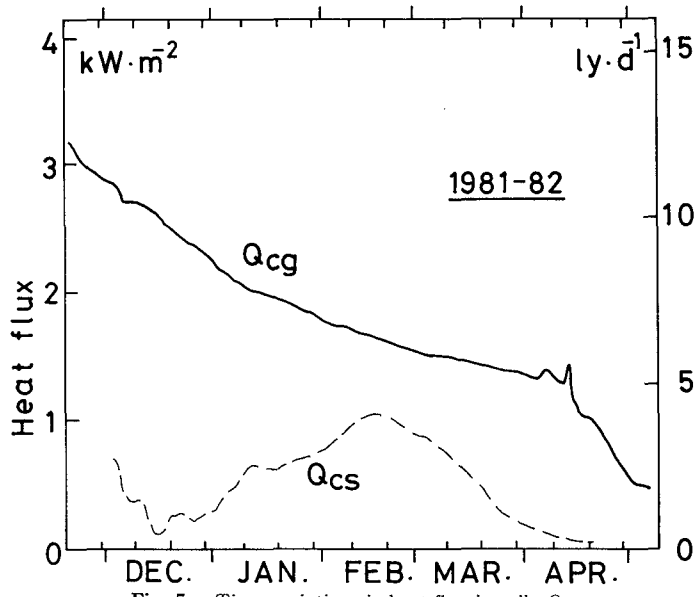

Fig. 7a Time variations in heat flux in soil, Q_{cg}, and in snow, Q_{cs} during the 1981–82 winter.

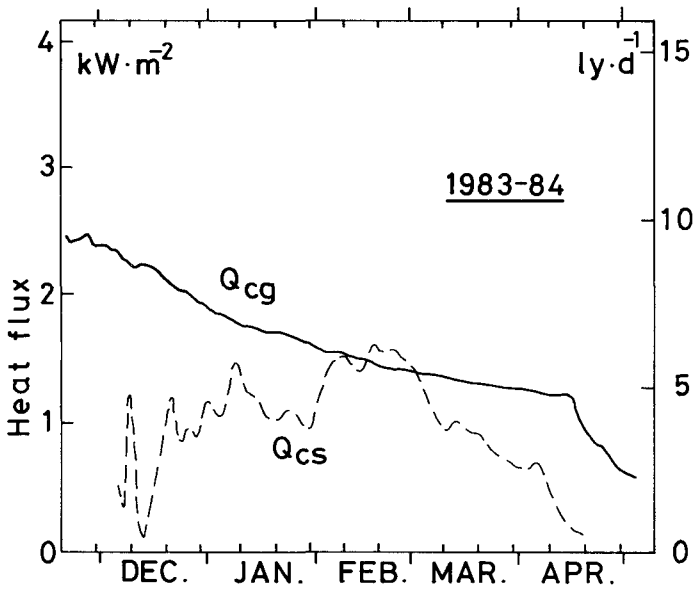

Fig. 7b. Time variations in heat flux in soil, Q_{cg}, and in snow, Q_{cs}, during the 1983–84 winter.

in Fig. 6 by a broken line) agrees well with the value measured by the lysimeter (a solid line in Fig. 6). Therefore, the heat balance method represented by Equation (4) can be employed to estimate the amount of bottom-melt in the entire watershed. In order to estimate the bottom-melt, Q_{cs} should be obtained as described above. As Fig. 7 shows, Q_{cs} was larger in the 1983–84 winter with less snow than in the 1981–82 winter. Fluctuations in Q_{cs} and air temperature seem coherent. Therefore, it is deduced that Q_{cs} is mainly dependent on the air temperature and snow depth. In the following section, the method for calculating Q_{cs} using air temperature and snow depth will be explained.

II. 4. 1 *Numerical calculation of heat flux in snowcover*, Q_{cs}

The equation of one-dimensional heat conduction is written as,

$$\rho_s C_{ps} \frac{\partial T}{\partial t} = \frac{\partial}{\partial z}\left(K \frac{\partial T}{\partial z}\right), \tag{5}$$

where ρ_s is the snow density, C_{ps} the specific heat of snow, T the snow temperature, t the time, K the thermal conductivity of snow, and z the height above the bottom of the snowcover. ρ_s and K are the functions of z. The numerical finite difference method used to solve Equation (5) is the implicit scheme of Crank-Nicholson. Equation (5) can be solved for T at any point (z, t).

a) INITIAL CONDITIONS

Snow temperature profiles obtained by snow pit observations were used as the initial conditions.

b) BOUNDARY CONDITIONS

1. Upper boundary of z (snow depth): Observed snow depth.
2. Snow temperature at bottom of snowcover: Melting point of ice (0°C) at any time.
3. Surface temperature of snowcover:

The surface temperature of the snowcover, T_0, was not measured, but the air temperature T_a was observed continuously. Ishikawa et al. (1984, 1985) observed hourly mean values of T_a and T_0 in Sapporo, Japan, which are plotted in Fig. 8. The linear regression line was obtained by the least squares method between T_a and T_0. The difference of T_a and T_0 depends on such variables as the wind speed, solar radiation and observed period. The same method was used to obtain the relationship between T_a and T_0 for this watershed (Ishikawa, 1977). The relationship for daily mean temperatures of T_a and T_0 is as follows:

$$T_0 = T_a - 3.0 \text{ [°C]}. \tag{6}$$

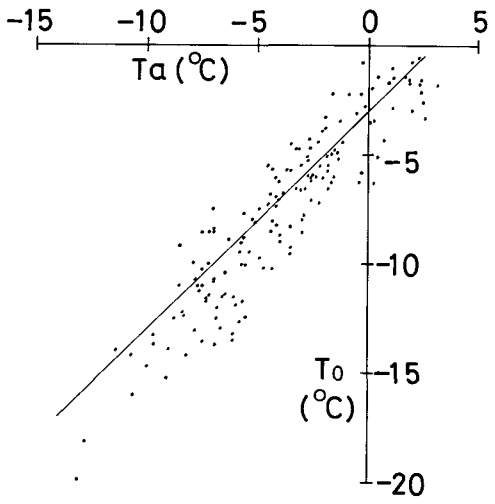

Fig. 8 Relation between daily mean air temperature, T_a, and daily mean surface temperature of the snowcover, T_0, in winter in Sapporo.

c) SNOW DENSITY PROFILES The snow density profiles can be calculated by the viscous compression theory of the snow layer (Kojima, 1957). The calculated density of the snow layer near the bottom of the snowcover did not agree well with the actual density profiles, because this layer consisted of coarse granular snow (Motoyama et al., 1985). Therefore, instead of applying the viscous compression theory, an empirical equation was obtained to relate the normalized height z' above the bottom of the snowcover to the snow density, $\rho_s(z')$, based on the density profiles obtained by the snow pit observations at the BH station during the 1981–82 and 1983–84 winters (Fig. 9).

For $HW > 22.5$

$$\rho_s(z') = (-0.35z' - 0.05F + 40)/(100 - F) \quad \text{for } z' \geq F,$$
$$\rho_s(z') = 0.40 \quad \text{for } z' < F, \tag{7a}$$

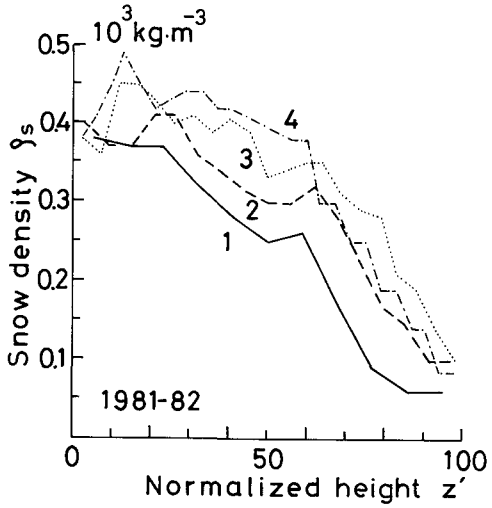

Fig. 9a Relation between the normalized height above the snow-ground interface, z', and the snow density, ρ_s, at BH station in the 1981–82 winter.

1. Dec. 4, 1981, solid line (snow depth: 1.09 m; snow water equivalent: 26.0×10kgm^{-2}; average snow density: 0.238×10^{3}kgm^{-3}).
2. Jan. 7, 1982, broken line (1.64, 48.4, 0.295).
3. Feb. 9, 1982, dotted line (2.07, 69.2, 0.334).
4. 4. Mar. 11, 1982, dash-dotted line (2.52, 84.4, 0.335,)

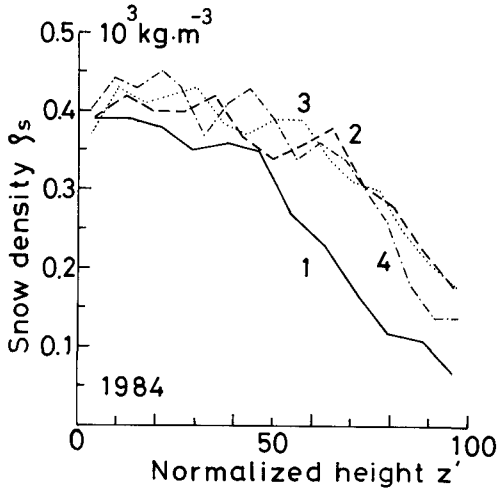

Fig. 9b Relation between the normalized height z' and the snow density ρ_s at BH station in the 1984 winter.

1. Jan. 13, 1984, solid line (1.22, 32.0, 0.262).
2. Feb. 15, 1984, broken line (1.33, 45.0, 0.338).
3. Mar. 7, 1984, dotted line (1.49, 51.4, 0.345).
4. Mar. 29, 1984, dash-dotted line (1.67, 57.9, 0.346).

where $F=(HW-22.5)/0.175$,

$$z'=100z/z_{\max}.$$

For $HW \leq 22.5$

$$\rho_s(z')=(-Bz'+0.05z'+100B)/100. \tag{7b}$$

where $B=(HW-2.5)/50$.

In the above equations $z_{\max}$ is the original snow depth, z the height above the bottom of the snowcover, and HW the total snow water equivalent. The unit of ρ_s is 10^3kgm^{-3} and that of HW is 10kgm^{-2}. The values of B and F are shown in Fig. 10. If HW is larger than 22.5× 10kgm^{-2}, the density of the snow layer between the bottom and point F is 0.4×10^{3}kgm^{-3}.

The density profile between point F and the surface layer is linear. If HW is smaller than $22.5\times10\text{kgm}^{-2}$, then the density of the bottom layer is B and that of the surface is $0.05\times10^{3}\text{kgm}^{-2}$. The density profile of the entire layer is linear for this case.

d) THERMAL CONDUCTIVITY OF SNOW, K

Izumi and Huzioka (1975) proposed the thermal conductivity of snow, K, as a function of snow density ρ_s as follows:

$$\log_{10}(4.19K) = -3.73 + 2.16\rho_s, \qquad (8)$$

where the units of ρ_s and K are 10^{3}kgm^{-3} and $10^{2}\text{Wm}^{-1}\text{K}^{-1}$, respectively.

e) SPACING WIDTH AND TIME INTERVAL FOR CALCULATION

Equation (5) is calculated numerically under the condition of the specific spacing width Δz(0.1 m) and time interval Δt(1 day and 10 days). Equation (5) converged easily under these conditions.

II. 4. 2 *Verification of method*

One example of the calculated snow temperature profile is shown in Fig. 11. The day on which simulation was started is January 1, 1982 (open circles show the initial temperature profile) and the time step is 1 day. In this figure, the profile calculated (crosses) is compared with the one observed by the snow pit observation on February 9, 1982 (solid line), and both agree well with each other. Thus this method for calculating snow temperature profile based on the air temperature and the snow depth is considered to be an appropriate method. Using

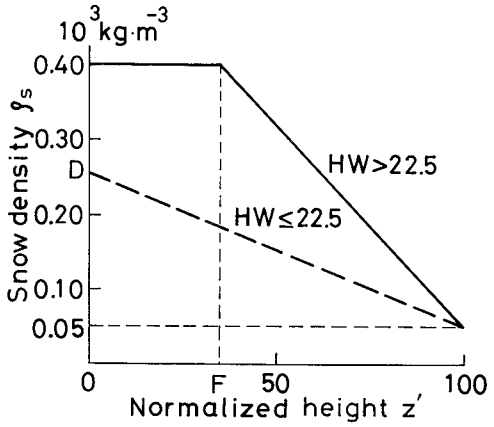

Fig. 10 Snow densities ρ_s as the functions of normalized height z' used in the experiment.

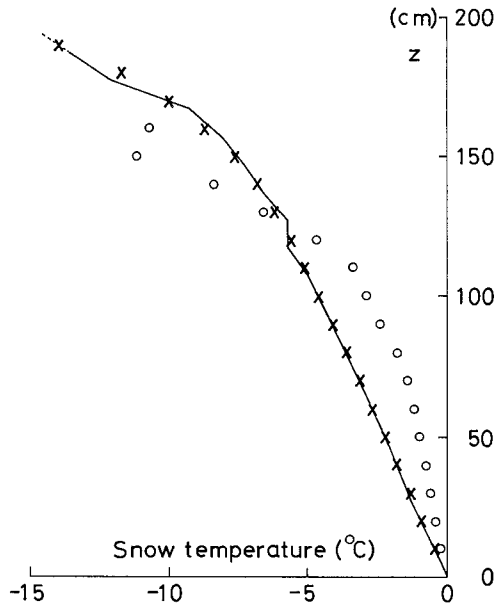

Fig. 11 An example of the profile of snow temperature calculated at BH station.
Open circles: initial temperature profile on Jan. 1, 1982.
Solid line: observed temperature profile on Feb. 9, 1982.
Crosses: calculated temperature profile on Feb. 9, 1982.

this temperature profile, Q_{cs} is easily calculated by Equation (9).

$$Q_{cs}=K\frac{\partial T}{\partial z}. \tag{9}$$

II. 5 *Bottom-melt in watershed*

A method for calculating Q_{cs} at a station was proposed in the previous section. For the purpose of estimating the contribution of the amount of bottom-melt to the rate of stream flow, it is necessary to estimate the amount of bottom-melt in the entire area of the watershed. In the following section, the method to calculate Q_{cs} for the entire watershed will be explained, followed by another section explaining the estimate of the total amount of bottom-melt in the watershed.

II. 5. 1 *Heat flux in snowcover, Q_{cs}, in watershed*

Data on snow depth and air temperature is necessary in order to estimate the Q_{cs} distribution in the watershed. Two assumptions are made here: (1) Since the daytime lapse rate of air temperature is about $0.6-1.0\times10^{-2}$ °Cm^{-1}, during the daytime, the air temperature at the lower region is 2 – 3 °C higher than that at the upper region. Radiative cooling often occurs at night in the lower region, but is much less in the upper region. Hence, at night, the air temperature is lower in the lower region than that in the upper region. Therefore, 10-day mean air temperatures are assumed to be the same at any place in the watershed. (2) The relationship between the altitude and the water equivalent of the snowcover is assumed to be linear (see section III. 2, Fig. 20). Therefore the distributions of snow depth and snow density can be calculated at any place using this relationship and the viscous compression theory of the snow layer (Motoyama and Kojima, 1985).

The observed snow depths (solid line) and calculated (open circles) for every five days at three locations are shown in Fig. 12. Small fluctuations in the observed snow depth are not reflected well by the calculated ones, but over all, the snow depth is satisfactorily simulated. The snow depth distribution with respect to the altitude is shown in Fig. 13. The abscissa in Fig. 13 represents both the ratio of the snow water equivalent at a point to that at BH station, and also corresponds to the altitude in the watershed. The ratio of the snow water equivalent in the 1981–82 winter with heavy snow ranges from 1.0 to 1.6. On the other hand, the ratio in the 1983–84 winter with light snow ranges from 1.0 to 2.0. These results indicate that a large difference exists in snow depth even in the small watershed (11.2km^2) with a small change in altitude (350m). Since the amount of bottom-melt depends on the snow depth, there might be a large variation in the amount of bottom-melt in the watershed.

The value of Q_{cs} was calculated for the altitude interval of 50 m with the time interval of 10 days and the spacing width of 0.1 m. Table 1 presents the monthly total of Q_{cs} at BH station and the areal mean in the watershed. The ratios, Q_{cs}(areal mean)/Q_{cs}(BH), ranged from about 0.8–0.9, except in December 1981. The ratio was slightly larger in the 1981–82

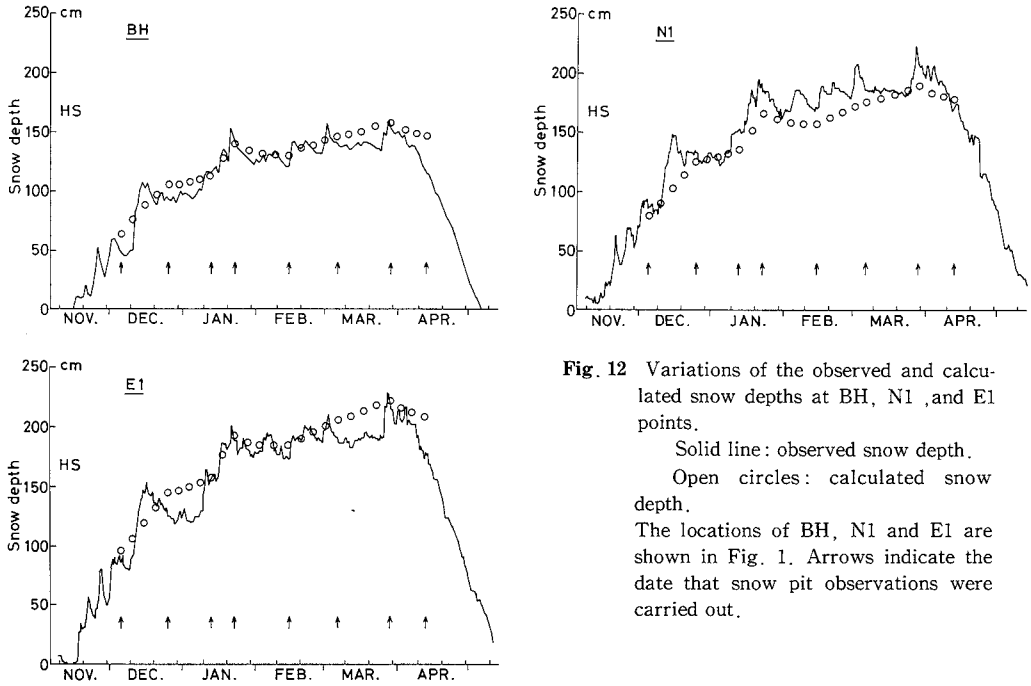

Fig. 12 Variations of the observed and calculated snow depths at BH, N1 ,and E1 points.
Solid line: observed snow depth.
Open circles: calculated snow depth.
The locations of BH, N1 and E1 are shown in Fig. 1. Arrows indicate the date that snow pit observations were carried out.

Table 1 Monthly heat flux in snow, Q_{cs} (in the unit of kJm^{-2}).

	Q_{cs} (BH)	Q_{cs} (areal mean)	Q_{cs} (areal mean) / Q_{cs} (BH)
December 1981	1.15	1.89	1.25
January 1982	2.90	2.49	0.86
February 1982	4.27	3.84	0.90
March 1982	2.82	2.49	0.88

	Q_{cs} (BH)	Q_{cs} (areal mean)	Q_{cs} (areal mean) / Q_{cs} (BH)
December 1983	3.69	3.18	0.86
January 1984	5.69	4.89	0.86
February 1984	6.84	5.20	0.70
March 1984	4.69	3.75	0.80

winter with deep snow than in the 1983−84 winter.

III. 5. 2 *Bottom-melt, M_b, in watershed*

The amount of bottom-melt, m_b, can be estimated from heat flux differences between the ground and the snowcover: $m_b(\mathrm{HF})=(Q_{cg}-Q_{cs})/L_m$. The value of Q_{cs} was obtained as described in the previous section. The heat flux in the ground Q_{cg} at any place in the

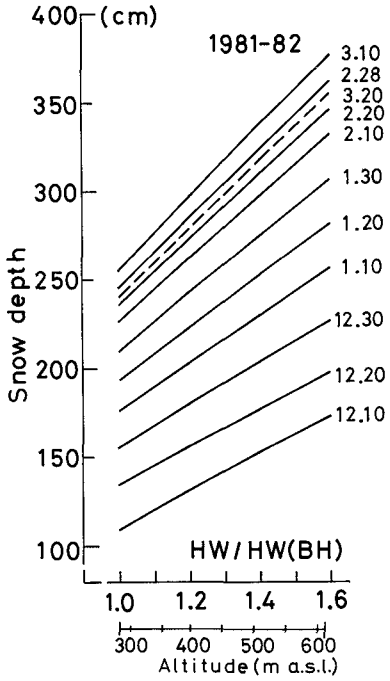

Fig. 13a Snow depth distributions for every ten days in the 1981–82 winter. The abscissa represents the ratio of the snow water equivalent at any place to that at BH station, which is related to the altitude in the watershed.

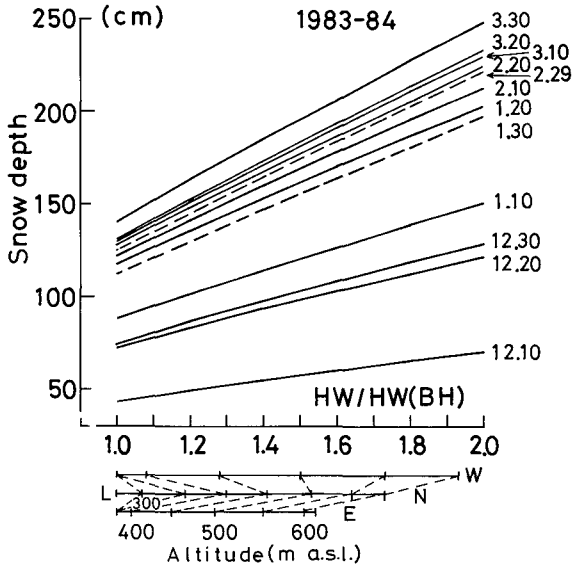

Fig. 13b Snow depth distributions for every ten days in the 1983–84 winter. The corresponding altitude is classified by four subwatersheds (see Fig. 20).

watershed was assumed to be the same as that at BH station, as shown in Fig. 7.

The calculated amount of bottom-melt, m_b(HF), is slightly different from the observed amount, m_b(LY), (see Fig. 6). Especially in February 1984, the values of m_b(HF) at BH station become negative for a short period, but no abrupt change is seen in the amount of runoff measured by the lysimeter, m_b(LY). This implies that the ground surface (bottom of the snowcover) is frozen at times. However, the frozen soil layer is shallow, only a few centimeter thick, and the percolation of meltwater continues below this frozen layer. Therefore, m_b(HF) does not always give a correct estimate of the amount of bottom-melt. Thus, the relationship between m_b(HF) and m_b(LY) was obtained in order to calculate the more realistic amount of bottom-melt from the heat balance calculation.

$$m_b(\mathrm{LY})=0.89m_b(\mathrm{HF})+0.03\,[\mathrm{mmd^{-1}}] \text{ for } 1981-82, \tag{10a}$$

$$m_b(\mathrm{LY})=0.74m_b(\mathrm{HF})+0.11\,[\mathrm{mmd^{-1}}] \text{ for } 1983-84. \tag{10b}$$

Different empirical formulae were obtained for different winters, because the perco-

lation rate of meltwater in the soil depends on the soil structure, the water content in the soil, and so on.

The estimated amount of bottom-melt for the areal mean in the watershed, which calculated from the areal mean M_b(HF) and Equation (10), is shown by the solid line in Fig. 14. The areal mean value M_b is slightly larger than m_b at BH station, as indicated by the

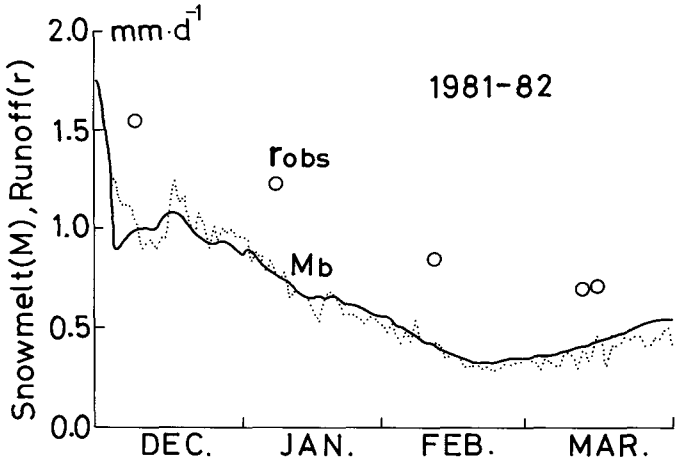

Fig. 14a Areal mean amount of bottom-melt and runoff in the 1981–82 winter.
Solid line: areal mean daily amount of bottom-melt.
Dotted line: daily amount of bottom-melt at BH station.
Open circles: daily amount of runoff depth.

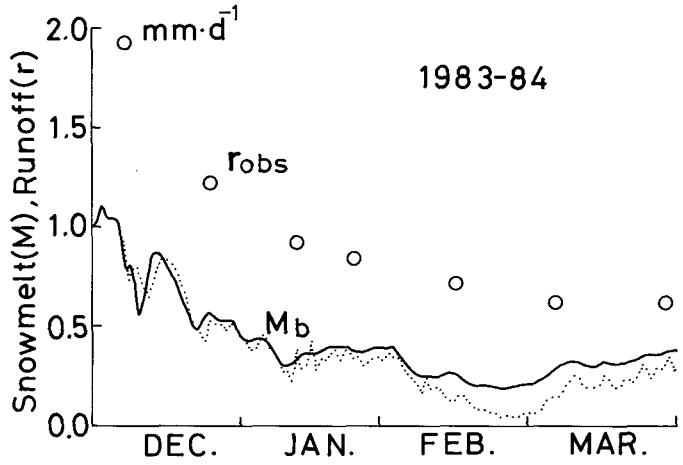

Fig. 14b Areal mean amount of bottom-melt and runoff in the 1983–84 winter. The notations are the same as in Fig. 14a.

dotted line. In the 1981−82 winter with heavy snow, the difference between M_b and m_b was small. However in the 1983−84 winter with light snow, the difference was large, especially in February.

II. 6 *Water balance*

The water balance of the watershed in winter is expressed as,

$$\Sigma M_b = \Sigma r + \Delta S_d, \tag{11}$$

where ΣM_b is the total amount of bottom-melt, Σr is the total amount of runoff depth and ΔS_d is the change in groundwater storage, which is obtained as a residual of this equation. These components are given in Table 2.

The value of ΔS_d was −34.4mm from January to March in 1982, and −40.5mm for the same period in 1984. These values indicate the loss of groundwater storage in winter. It is clearly shown that the amount of bottom-melt supplies about one half of the runoff of the watershed. This might be the main reason for the larger specific runoff in the snowy area than that in the snow-free area as reported by Arai (1980).

Snow does not melt at the bottom of the snowcover in the ground-frozen watershed. Therefore stream water is only supplied by a discharge from the groundwater storage, which have been cultivated before the freezing of the ground.

Table 2 Monthly values of water balance components (mm-water). ΣM_b is the amount of bottom-melt, Σr is the amount of runoff depth and ΔS_d is the change in groundwater storage.

	ΣM_b	Σr	ΔS_d	$\Sigma M_b/\Sigma r$
December 1981	(30.1)			
January 1982	21.1	34.9	−13.8	0.60
February 1982	10.8	23.1	−12.3	0.47
March 1982	13.8	22.1	−8.3	0.62
January-March 1982	45.7	80.1	−34.4	0.57

	ΣM_b	Σr	ΔS_d	$\Sigma M_b/\Sigma r$
December 1983	(19.8)			
January 1984	11.9	29.3	−17.4	0.41
February 1984	7.1	20.8	−13.7	0.34
March 1984	9.8	19.2	−9.4	0.51
January-March 1984	28.8	69.3	−40.5	0.42

II. 7 *Method for calculating runoff*

A "tank model" was used to calculate the amount of runoff during the snowy season (Sugawara et al., 1984). A series of two tanks of the storage type was adopted (Fig. 15),

in which the upper tank had two outlets, one on the side for the runoff and another on the bottom for infiltration; the lower tank consisted of one outlet for the runoff. It was assumed that the amount of bottom-melt, M_b, is supplied to the tank every day, and the calculated amount of runoff, r, is discharged from the outlets on the side. The equations used are:

$$r(i)=0.04DA(i)+0.008DB(i) \quad [\mathrm{mmd^{-1}}], \tag{12a}$$

$$DA(i+1)=DA(i)+M_b(i+1)-(0.04+0.03)DA(i) \quad [\mathrm{mm}], \tag{12b}$$

$$DB(i+1)=DB(i)+0.03DA(i)-0.008DB(i) \quad [\mathrm{mm}], \tag{12c}$$

where i is the time step, and DA and DB are the heights of storage in the upper and lower tanks, respectively. The parameter of the tank structure was determined by referring to the recession rates of the runoff hydrograph (Fig. 16).

Using the tank model, the hydrographs from December 1 to March 31 in both the 1981–82 and the 1983–84 winter were calculated. The initial heights of storage water, DA and DB, in the tanks were determined by the trial and error method until the calculated amount of discharge fitted well to the observed amounts. The best fit values of DA and DB are shown in Table 3. The initial value of DA for the upper tank was less in 1981–82 than that in 1983–84. In November 1981, the air temperature was low, and snow started accumu-

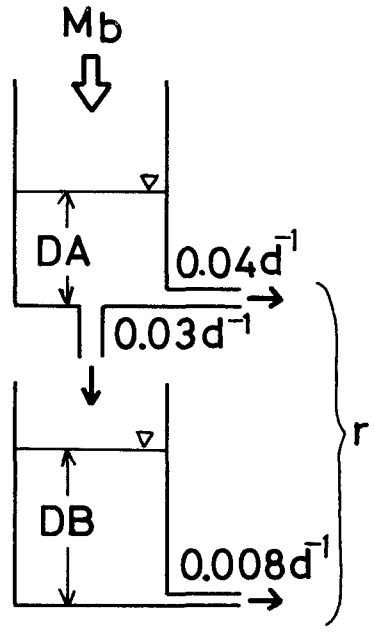

Fig. 15 Derived tank model. The coefficients of tank's outlet are shown in the unit of d^{-1}.

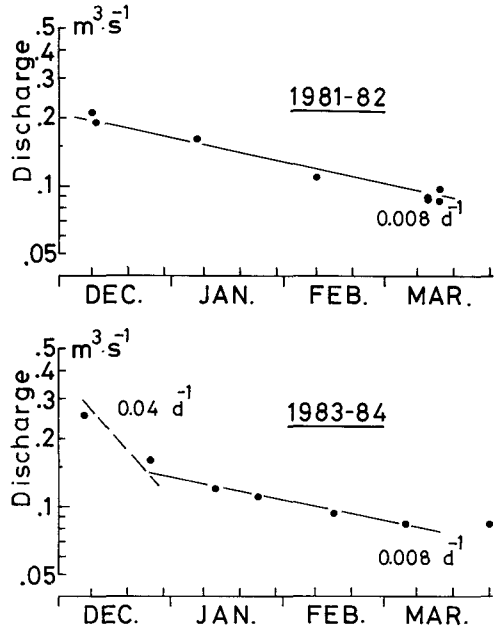

Fig. 16 Recession curves for runoff hydrographs in the 1981–82 and the 1983–84 winter.

Table 3 Amount of initial storage of water (in mm) in the tank model (Fig. 15).

	Dec. 1, 1981	Mar. 31, 1982	Dec. 1, 1983	Mar. 31, 1984
DA	26	6	40	4
DB	80	53	80	49

lating relatively earlier than usual. On the other hand, in November 1983 the air temperature was high and rain water was supplied to the watershed. Therefore, it is deduced that the initial water storage of the upper tank, DA, might be dependent on the groundwater storage, which has resulted from the hydrological events in the previous period.

The observed and the calculated hydrograph are plotted in Fig. 17. The open circle, thick solid line and thin broken line represent the daily amount of runoff depth observed, r_{obs}, that of runoff depth calculated, r_{cal}, and that of runoff depth from the outlet of the lower tank calculated, respectively. The observed hydrograph was simulated well by the tank model. The rate of bottom-melt, M_b, (also shown in Fig. 17 by broken line) shows short-period fluctuations, but the calculated runoff depth decreases steadily. It is reasonable to assume that the runoff depth from the lower tank corresponds to the constant groundwater flow from the deep layer, while the runoff depth from the upper tank is the groundwater flow from the shallow layer.

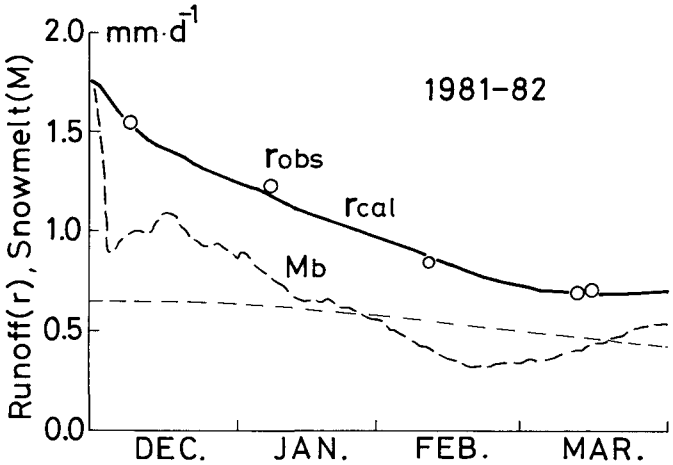

Fig. 17a. Areal mean amount of bottom-melt and the simulated amount of runoff in the 1981−82 winter.

Thick broken line: areal mean daily amount of bottom-melt, M_b.

Open circles: daily amount of runoff depth observed, r_{obs}.

Solid line: daily amount of runoff depth calculated, r_{cal}.

Thin broken line: amount of runoff depth only from the outlet of the lower tank (see Fig. 15).

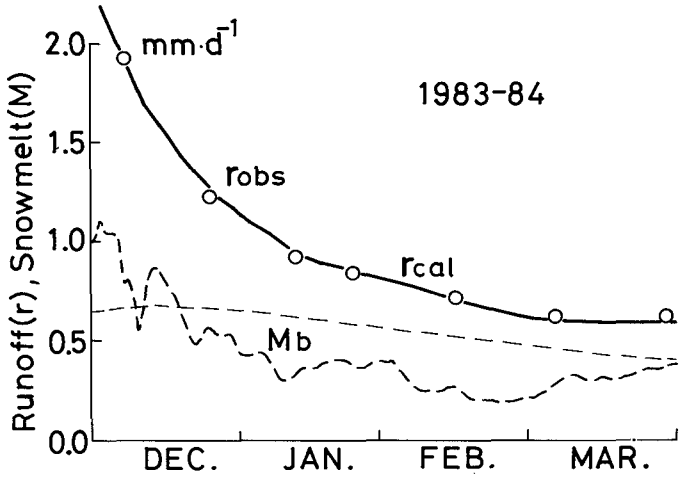

Fig. 17b Areal mean amount of bottom-melt and the simulated amount of runoff in the 1983–84 winter. The notations are the same as in Fig. 17a.

On the other hand, in the case of no bottom-melt the runoff depth was also calculated using the same runoff model without supplying bottom-melt to the tank. This result is shown in Fig. 18. The runoff from the upper tank disappears in mid-February. The amount of runoff depth with no bottom-melt is one half of the observed runoff depth in March. This suggests that the amount of bottom-melt plays an important role in the river runoff in winter. Therefore, the bottom-melt cannot be ignored in the water balance of an area with deep snow.

In snowy regions it is difficult to measure the amount of stream discharge in winter because the river surface is usually covered with snow and ice. But the amount of runoff can be estimated or predicted using the method described above in order to make an efficient use of low-water flow in winter.

II. 8 *Conclusion*

The amount of snowmelt at the bottom of the snowcover as well as the amount of runoff of a watershed was studied for the two winter seasons. The following results were obtained.

1. The observed amount of bottom-melt was dependent upon the air temperature and the snow depth. Using this relationship, the areal amount of bottom-melt was estimated using the heat balance at the snow-ground interface.

2. A runoff tank model was developed and it simulated well the amount of runoff of the watershed in winter.

3. The amount of bottom-melt supplied about one half of the amount of runoff in the

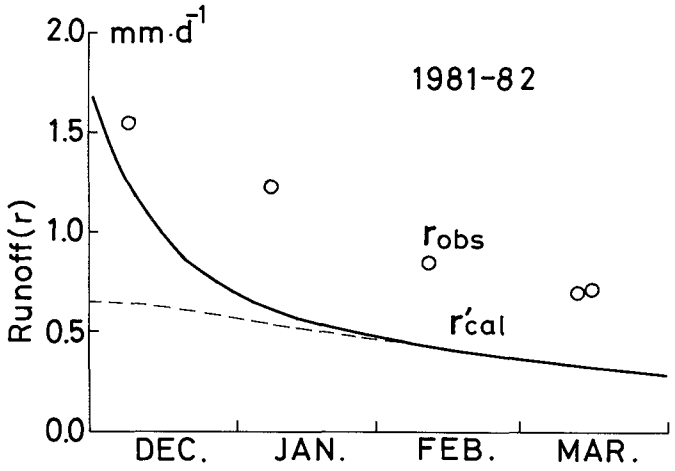

Fig. 18a Simulated amount of runoff in the case of no bottom-melt in the 1981–82 winter.
Open circles: daily amount of runoff depth observed, r_{obs}.
Solid line: daily amount of runoff depth simulated, r'_{cal}.
Broken line: amount of runoff depth from the outlet of the lower tank (see Fig. 15).

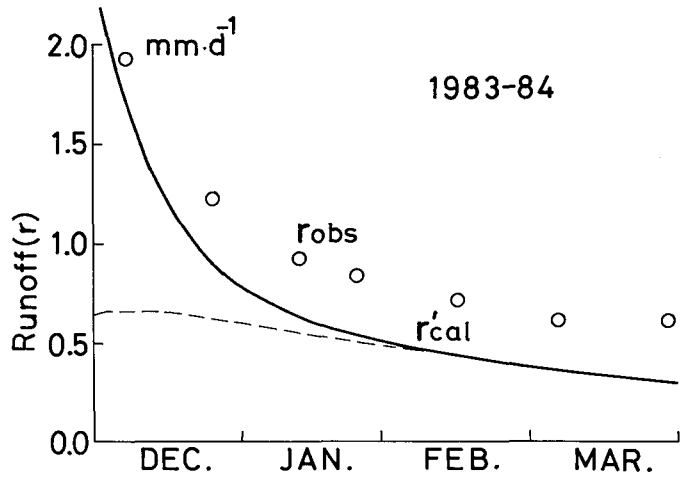

Fig. 18b Simulated amount of runoff in the case of no bottom-melt in the 1983–84 winter. The notations are the same as in Fig. 18a.

watershed. This indicates that the bottom-melt plays an important role in the water balance during the winter.

III. Snowmelt runoff in snowmelt season, 1. daily analysis

III. 1 *Introduction*

The total amount of snow covering the ground immediately before the snowmelt season in a watershed has been measured by many investigators with an attempt to forecast the amount of snowmelt runoff (Leaf, 1971; Rango, 1983; Sugawara et al., 1984). A prerequisite for this forecasting is to find out the water balance in the watershed, but many points remain unknown in this respect. The number of papers which discuss the water balance on the basis of the observed amounts of snowmelt and runoff in the watershed is only a few (Ono and Kawaguchi, 1974; Motoyama et al., 1986b).

The present study was conducted (1) to clarify the water balance in a watershed during the snowmelt season on the basis of observed hydrological data; and (2) to develop a method for calculating the daily amount of snowmelt runoff.

III. 2 *Instrumentation*

Observed periods were from April to June in the years, 1981, 1982, 1983, and 1984. The objects observed and the instruments used were: (1) Snow water equivalents, HW, in the watershed. They were measured at about 20 sampling points in the watershed (Fig. 1) in mid-April each year. At a sampling point, the average snow depth, $\overline{HS}$, was obtained using about ten snow sondes. The average snow density, $\bar{\rho}_s$, was calculated from three or four measurements by a snow sampler. Then, the snow water equivalent at a station was calculated by the equation: $HW=\overline{HS}\,\bar{\rho}_s$. (2) Amounts of snowmelt in the watershed. They were measured also at the same points as in (1) in the watershed (Fig. 1). The height of snow depth, HS, and snow densities, ρ_s, between the snow surface and 0.05 m below the snow surface, and between 0.05 m and 0.10 m below the snow surface were measured from time to time. Therefore the snowmelt amount between the two measurements was calculated by the equation $m=\Delta(HS)\,\rho_s$, where $\Delta(HS)$ is the decrease in snow depth between the two measurements. (3) Melting rates at BH station. Melting rates were continuously observed by four different methods (Fig. 19); including, the snow stake method, the lysimeter method, snow pit observations and the heat balance calculations described in Section I.3. The details of them were described by Motoyama et al. (1983a, b). (4) Stream discharge. The water level was continuously measured by the water level recorder. To establish a formula for the conversion of the water level to the discharge, the discharges were observed at the outlet of the watershed once or twice a day every snowmelt season by

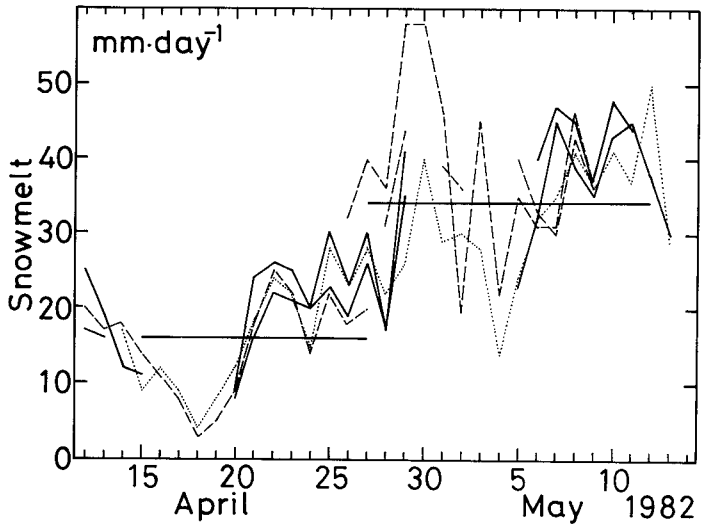

Fig. 19 Daily amount of snowmelt obtained by four different methods.
Solid line: snow stake method.
Broken line: lysimeter method.
Horizontal thick solid line: snow pit observations.
Dotted line: heat balance method.

measuring the vertical cross sectional area and the flow velocity of the river. (5) Meteorological observations. Air temperature, wind speed, solar radiation, reflected solar radiation, net radiation, surface temperature, vapor pressure and precipitation were continuously observed at BH station.

III. 3 *Water balance during snowmelt season*

The water balance was calculated from the date when the snow survey was started to the date when all the snow disappeared from the watershed.

III. 3. 1 *Water balance equation*

The water balance of the watershed for the snowmelt season is written as,

$$\Sigma M+\Sigma P=\Sigma r+\Delta E+\Sigma ET+\Delta S_a, \tag{13}$$

where ΣM is the total amount of snowmelt (the total amount of snow water equivalent on the beginning date of calculating the water balance), ΣP is the total precipitation, Σr is the total amount of runoff depth, ΔE is the amount of mass transfer at the snow surface (evaporation: +; condensation: −), ΣET is the total amount of evapotranspiration in the watershed, ΔS_a is the change in groundwater storage and the change of water storage in the unsaturated zone (gain: +; loss: −).

III. 3. 2 *Each component*

The snow water equivalents, *HW*, obtained at about 20 points in the watershed are plotted against the altitude, h, in Fig. 20. Linear relationships, which were classified into four sub-watersheds (West, North, East and Lower regions) were obtained except in 1982 (a heavy snow season). The altitudinal distribution of sub-watershed area, $A(h)$, is shown in Fig. 21. The total amount of snow water equivalent can be calculated as follows:

$$HW_{\text{total}} = \int HW(h)A(h)\mathrm{d}h. \tag{14}$$

The total amount of snow water equivalent in the watershed (including rain water) was

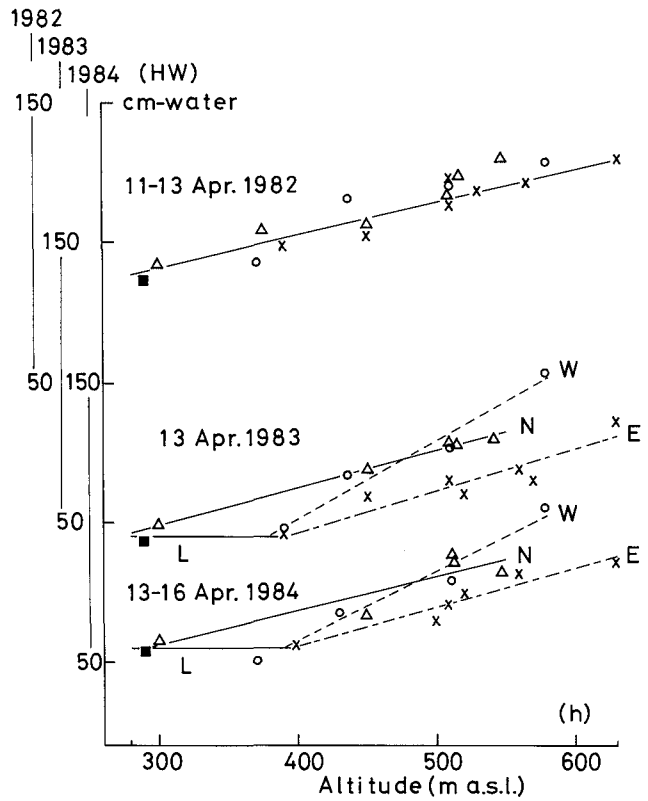

Fig. 20 Altitudinal distribution of snow water equivalents in 1982, 1983, 1984. Linear regression lines between the altitude and snow water equivalent were obtained for four sub-watersheds, except in 1982.

Open circles: west; open triangles: north; crosses: east; solid squares: lower region.

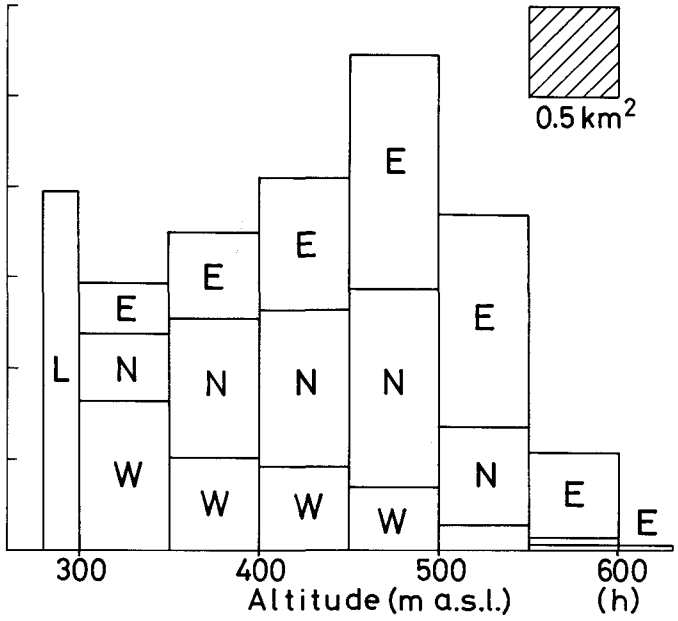

Fig. 21 Altitudinal distribution of sub-watershed area. Square of oblique lines indicates the area of 0.5km² (W : west ; N : north ; E : east ; L : lower region).

1.34×10^7m³-water (areal mean : 120 cm-water) in 1982, a heavy snow season, but during the seasons of light snow, 1983 and 1984, it was 7.6×10^6m³-water (68cm-water) and 7.8×10^6m³-water (70 cm-water), respectively.

Each of P, E and ET was assumed to be the same at any place in the watershed ; P was observed at BH station ; E was calculated by an empirical formula using the meteorological data at BH station (see Section IV. 2) ; and ET was assumed to be 0 mmd^{-1} before the date one week after snow disappeared in the lower region, and 1 mmd^{-1} after that date (Arai, 1980).

The total amount of snowmelt runoff, Σr, was calculated by two methods. The one method is to sum up the individual amounts of runoff simply throughout the snowmelt season, while the other is to sum them up considering the recession curve on the runoff hydrograph, indicated by the area covered by oblique lines in Fig. 22.

III. 3. 3 *Results*

Each component of the water balance is represented in Table 4 and the runoff coefficients are shown in Table 5. The results show that 80 − 100 % of the snowcover in the watershed ran off as stream flow in these three seasons, and the runoff coefficient was not

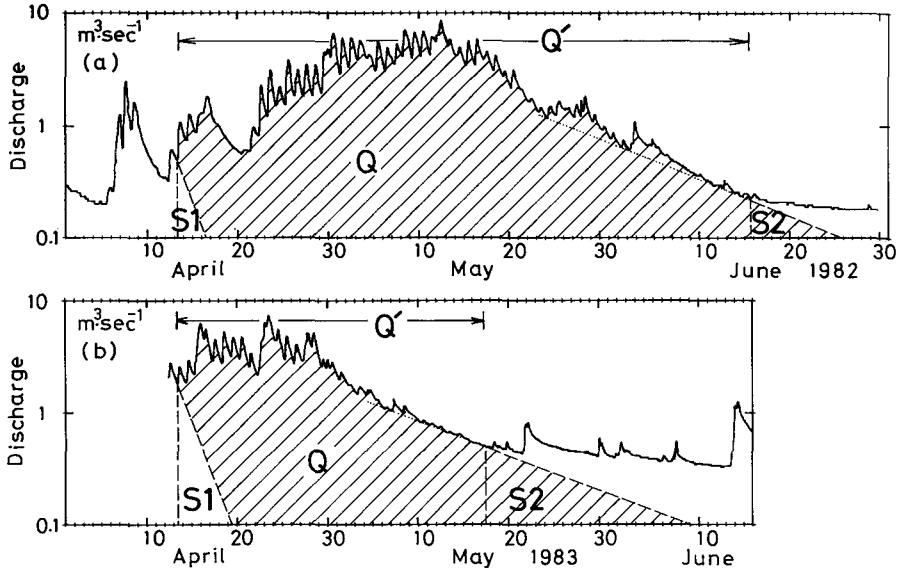

Fig. 22 Runoff hydrographs in 1982 and 1983. The area of oblique lines indicates the amount of separated snowmelt runoff: $Q=Q'+S2-S1$. The values of Q, Q', $S2$, and $S1$ are shown in Table 5.

Table 4 Water balance: $\Sigma M+\Sigma P=\Sigma r+\Delta E+\Sigma ET+\Delta S_d$, where ΣM: total amount of snowmelt, ΣP: total amount of precipitation, Σr: total amount of runoff, ΔE: amount of evaporation or condensation at the snow surface, ΣET: estimated total amount of evapotranspiration, ΔS_d: estimated change in groundwater storage (in the unit of cm-water).

	ΣM	ΣP	Σr	ΔE	ΣET	ΔS_d	$\Sigma r/(\Sigma M+\Sigma P)$
Apr. 13-Jun. 15, 1982	106	14	110	1	2	7	0.92
Apr. 13-May. 30, 1983	60	13	68	0	2	3	0.93
Apr. 14-Jun. 4, 1984	67	3	53	−1	2	16	0.76

Table 5 Runoff coefficients of the snowcover in the watershed. $S1$, $S2$, Q' are shown in Fig. 22. Q: amount of snowmelt runoff, M: amount of snowmelt, P: amount of precipitation(in the unit of cm-water).

	$S1$	$S2$	Q'	$Q=Q'+S2-S1$	$M+P$	$Q/(M+P)$
1982	1	2	110	111(1)	120	0.93
1983	3	5	62	64(2)	68	0.94
1984	1	4	53	56(3)	70	0.80

(1) Apr. 13-Jun. 15 (2) Apr. 13-May. 17
(3) Apr. 14-Jun. 4

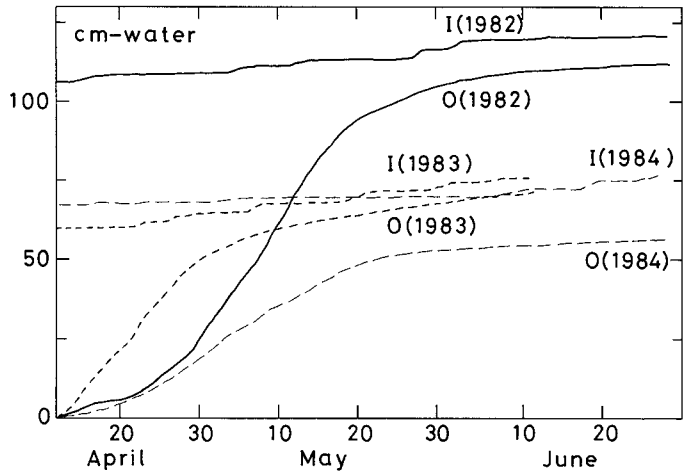

Fig. 23 Amount of integrated runoff depth, O, and amount of integrated precipitation in addition to areal mean snow water equivalent, I. Integration started on April 13.
Solid line: 1982; thick broken line: 1983; thin broken line: 1984.

dependent on the amount of snow during the season (Fig. 23). One characteristic of the water balance during the snowmelt season is that the loss of water from the surface of the watershed (evapotranspiration, etc.) is less than that during the snow-free seasons (Arai, 1980).

The total amount of mass transfer at the snow surface was found to be less than 2 % of the input (amount of snowmelt plus rain) to the watershed during the snowmelt season. The reason for this might be that loss by evaporation or sublimation during daytime was usually compensated for a gain due to condensation or sublimation during nighttime.

III. 4 *Characteristics of water balance in middle of snowmelt season*

The water balance in the middle of the snowmelt season on the watershed is written as,

$$\Sigma M+\Sigma R=\Sigma r+\Delta E+\Delta S_d+\Delta S_d', \tag{15}$$

where ΣR is the total amount of rainfall, $\Delta S_d'$ is the change in liquid water storage in the snowpack, and all the others were explained in the previous section.

The amount of snowmelt in the watershed was obtained by the snow stake method ($m=\Delta(HS)\,\rho_s$, see Section III.2) along with the altitudinal distribution of sub-watershed areas (Fig. 21). Examples of a time variation in snow depth are shown in Fig. 24. The altitudinal difference between the top and the bottom of the watershed is only 350 m, but the difference in snow depth between them is more than 1 m. The components of the water

balance are represented in Table 6. In the middle of the snowmelt season when the melting rates are 20 – 40 mmd^{-1} (Fig. 19), the amount of accumulated snowmelt ($\Sigma M+\Sigma R$) equals the amount of accumulated snowmelt runoff, Σr ; and the small values of ΔS_d and $\Delta S_d'$ indicate no change in the amount of liquid water storage in the snowpack and groundwater storage in the watershed.

Table 6 Water balance in the middle of the snowmelt season: $\Sigma M+\Sigma R=\Sigma r+\Delta E+\Delta S_d+\Delta S_d'$ where ΣM : total amount of snowmelt, ΣR : total amount of rain, Σr : total amount of runoff, ΔE : amount of evaporation or condensation at the snow surface, ΔS_d : change in groundwater storage, $\Delta S_d'$: change in liquid water storage in a snowpack (in the unit of cm-water)

	ΣM	ΣR	Σr	ΔE	$\Delta S_d+\Delta S_d'$	$\Sigma r/(\Sigma M+\Sigma R)$
Apr. 24–Apr. 29, 1982	12.1	0.3	9.6	0.0	2.8	0.77
Apr. 29–May. 10, 1982	39.4	2.6	40.8	0.3	0.9	0.97
Apr. 16–Apr. 19, 1983	11.2	0.3	11.4	−0.2	0.3	0.99

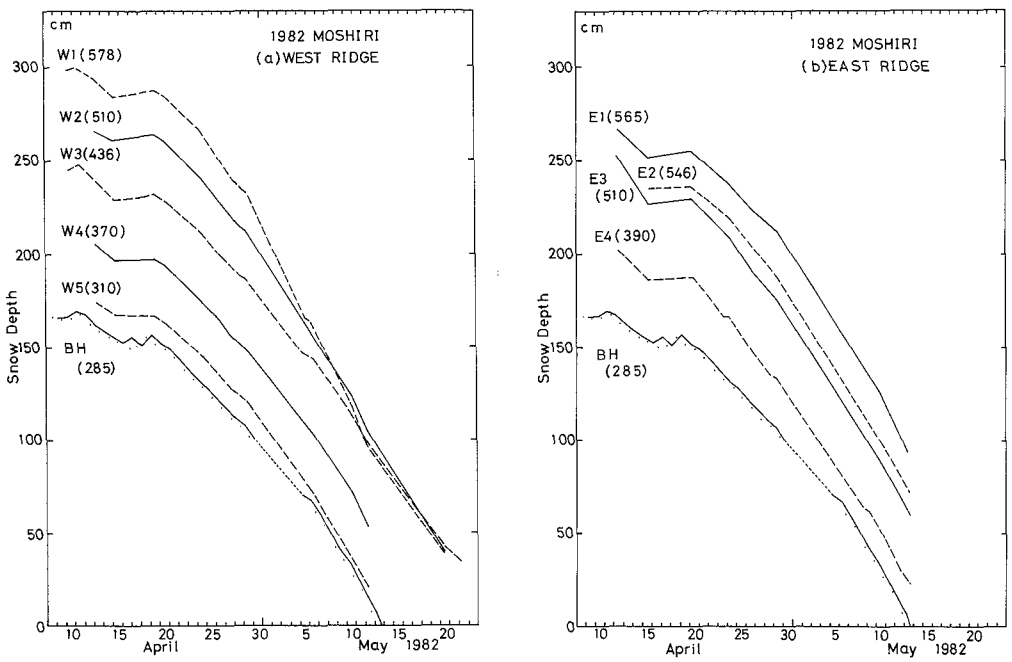

Fig. 24 Variations in snow depth in 1982. The number in parentheses indicates the altitude of the site. The locations of the sites are shown in Fig. 1.

III. 5 *Method for calculating daily snowmelt runoff*

A runoff model was devised for the snowmelt season in 1982 and subjected to a test as to its validity during the same period in 1981 and 1983.

III. 5. 1 *Determination of daily amount of snowmelt*

The daily amount of snowmelt obtained by four different methods at BH station differed from each other (Fig. 19). These differences seemed to be due to the variation in the horizontal structure of the snowcover from one place for one method to another place for another method. However, the amount of snowmelt that accumulated for several days did not vary according to the method (Motoyama et al., 1983b). In order to determine the daily amount of snowmelt at BH station, the snow stake method results were primarily used.

The total amount of snowmelt in the watershed was determined on the basis of the amount of snowmelt at BH station. Usually this amount at BH station is nearly equal to its areal mean value of the watershed (Kojima et al.; 1970, 1971). However, in 1982 the rate of snowmelt was larger in the upper region than in the lower region for such a long period as from April 12 to May 12 (Motoyama et al., 1983a; also see Fig. 24). The areal mean amount of snowmelt in the watershed was 1.1 times the amount of snowmelt at BH station.

After the snowcover disappeared at BH station in the lower region, the areal mean amount of snowmelt was estimated as follows: On an assumption of the constant rate of snowmelt in the entire watershed, the amount of snowmelt was obtained by an empirical formula using the mean daily air temperature at BH station (Kojima et al., 1983). This amount of snowmelt was multiplied by the ratio of the remaining area of the snowcover to the total area of the watershed (Fig. 25) in order to obtain the areal mean amount of snowmelt.

The results are shown in Fig. 26, where the broken line shows the amount of snowmelt estimated plus the amount of rainfall measured and the solid line shows the amount of snowmelt runoff observed. In the early snowmelt season the amount of snowmelt plus rain was larger than the amount of runoff. In the middle of the snowmelt season, the amount of snowmelt plus rain was nearly equal to the amount of runoff, as was discussed in Section III. 3. At the end of the snowmelt season, the amount of snowmelt plus rain was smaller than the amount of runoff. This phenomenon might be dependent

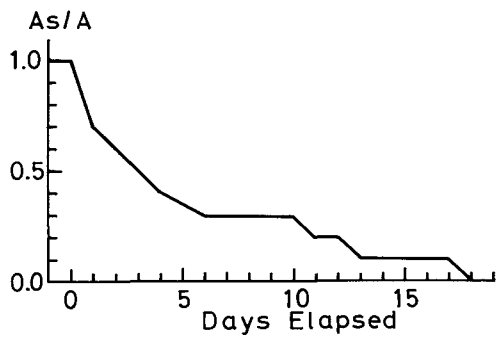

Fig. 25 The ratio of the remaining area of the snowcover to the total watershed area, A_s/A, with respect to the elapsed time, given in days, after the date that the snowcover disappeared in the lower region.

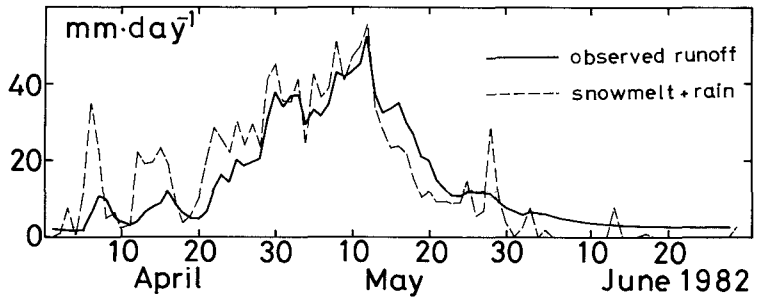

Fig. 26 Areal mean daily amount of snowmelt plus daily amount of precipitation (broken line), and daily amount of runoff depth (solid line) in 1982.

on a change in the amount of water stored in the snowpack, soil and groundwater.

III. 5. 2 *Determination of runoff model*

The runoff tank model (Fig. 27) was devised to calculate the daily amount of runoff. The daily amount of input water (snowmelt + rain), M, was supplied to the upper tank every day and the amount of runoff water, r, was discharged from the outlets on the side. The recession rates of the recession curves in a runoff hydrograph (Fig. 28) were determined by referring to the runoff coefficients of the tanks' outlets. The equations used are:

$$r(i)=0.25(DA(i)-90)+0.04DA(i)+0.01DB(i) \quad \text{for } DA(i)\geq 90\text{[mm]},$$
$$r(i)=0.04DA(i)+0.01DB(i) \quad \text{for } DA(i)<90\text{[mm]}, \tag{16a}$$
$$DA(i+1)=DA(i)+M(i+1)-0.25(DA(i)-90)-(0.04+0.01)DA(i) \quad \text{for } DA(i)\geq 90\text{[mm]},$$
$$DA(i+1)=DA(i)+M(i+1)-(0.04+0.01)DA(i) \quad \text{for } DA(i)<90\text{[mm]}, \tag{16b}$$
$$DB(i+1)=DB(i)+0.01DA(i)-0.01DB(i), \tag{16c}$$

where i is the time step, DA the height of storage in the upper tank and DB that in the lower tank. The units of r and M are both mmd^{-1} and the unit of DA and DB are both mm. This runoff tank model was nearly equal to the model in winter (see Fig. 15) for substantially small discharges. The amount of evapotranspiration was assumed to be 0 mmd^{-1} before the date one week after snow disappeared in the lower region, and 1 mmd^{-1} after that date (Arai, 1980).

III. 5. 3 *Results*

The observed and the calculated hydrograph in 1982 are plotted in Fig. 29a, where the solid line indicates the observed amount of runoff and the broken line the calculated one. Without changing the calculating method, the simulations of the daily amount of snowmelt

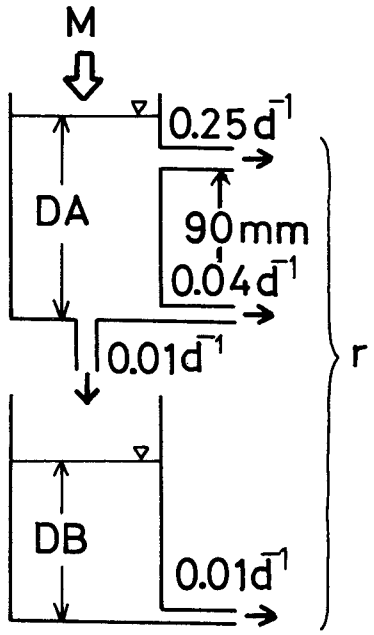

Fig. 27 Derived tank model. The coefficients of tank's outlet are shown in the unit of d^{-1}.

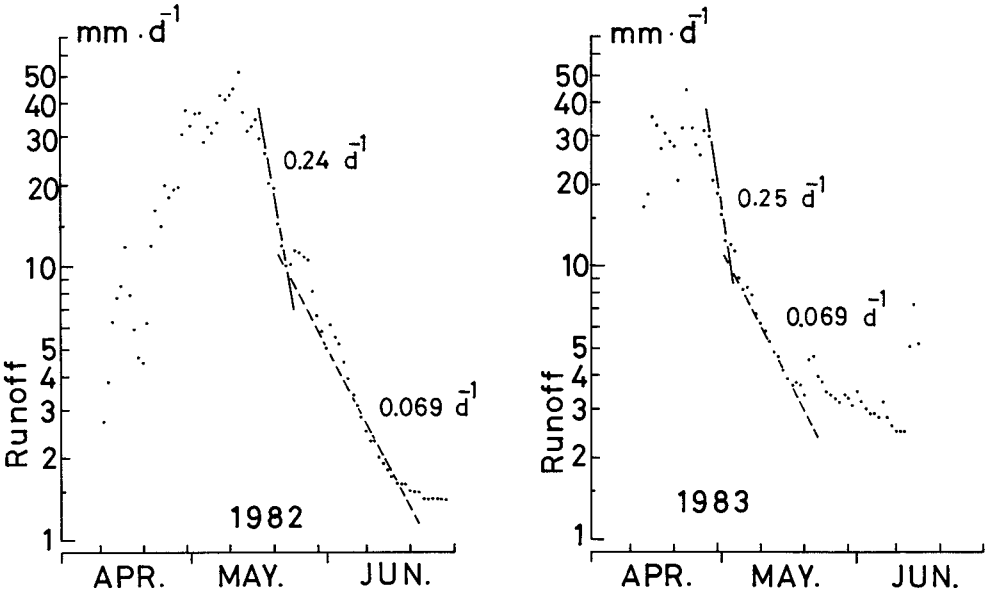

Fig. 28 Daily runoff hydrographs in 1982 and 1983 with the regression line and its slope.

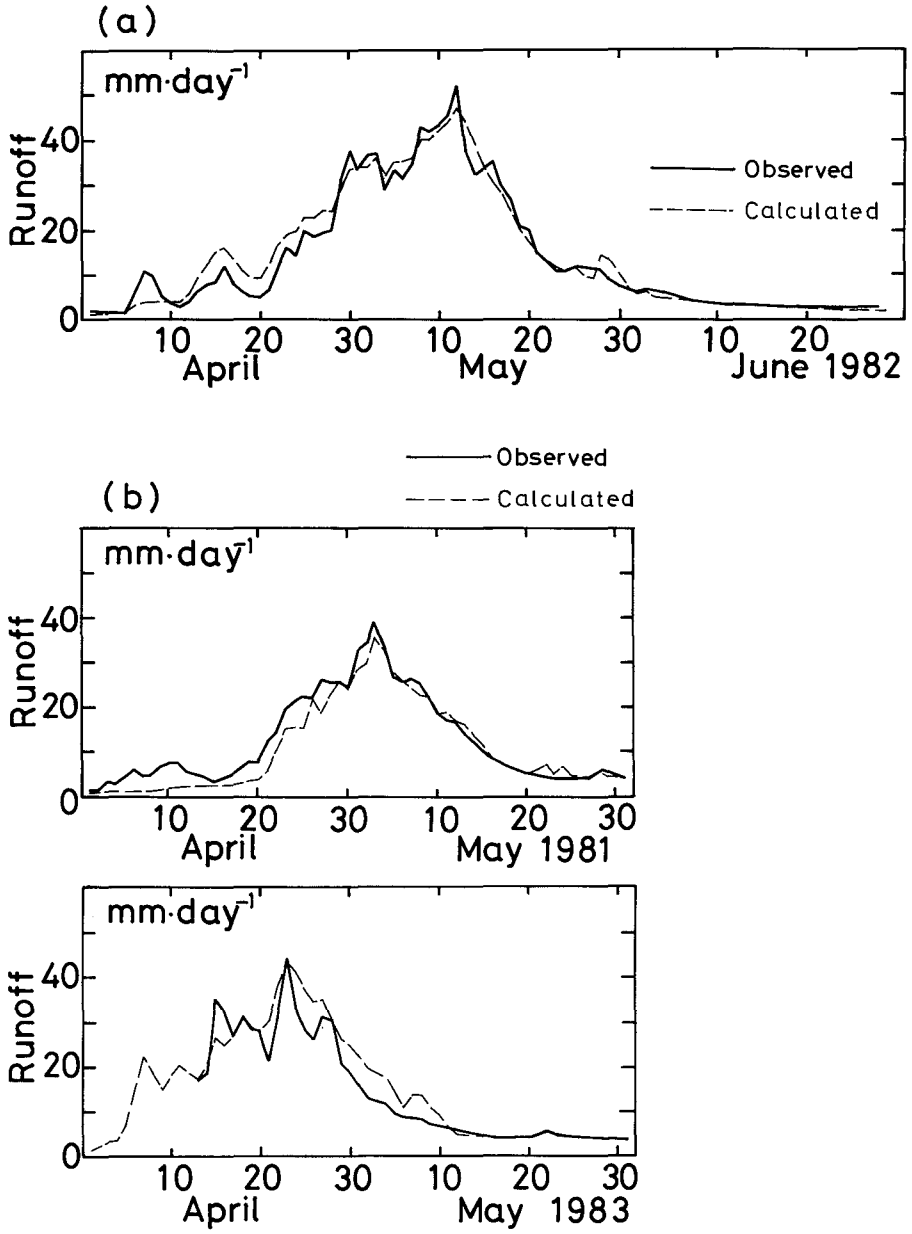

Fig. 29 Daily runoff depth in 1982 (a) and 1981, 1983 (b).
Solid line: observed runoff depth.
Broken line: calculated runoff depth using the tank model shown in Fig. 27.

runoff were made successfully in both 1981 and 1983 (Fig. 29b). An analogy between the tank structure and the runoff process was considered as follows: The upper and the lower tanks have two and one outlets for runoff, respectively. The runoff coefficients of these outlets were determined by the recession rates of the hydrograph at various ranges of amounts of runoff. It seems that the amount of runoff from the lower tank corresponds to the amount of groundwater flow from the deep layer, and that from the upper tank corresponds to the amount of groundwater flow from the shallow layer or the amount of surface runoff.

III. 6 *Conclusion*

The snow water equivalent, the snowmelting rate, and the stream discharge were measured at a watershed during four snowmelt seasons. Analysis was made of the water balance and runoff on the basis of observed hydrological data. The following results were obtained.

1. Ninety percent of the snowcover in the watershed ran off in years with heavy snow as well as in years with light snow.

2. The total amount of mass transfer at the snow surface was estimated to be less than 2 % of the input (amount of snowmelt plus rain) of the watershed during the snowmelt season.

3. In the middle of the snowmelt season, the melting rates were $20 - 40\ \mathrm{mmd^{-1}}$, and the amount of snowmelt was nearly equal to the amount of snowmelt runoff without a change in the amount of groundwater storage.

4. A tank model was devised to calculate the amount of snowmelt runoff. The simulation of daily amount of snowmelt runoff was made successfully for three years without changing the tank structure.

IV. Snowmelt runoff in snowmelt season, 2. hourly analysis

IV. 1 *Introduction*

The daily amount of runoff in the snowmelt season can be forecasted by the runoff model described in the previous chapter. For forecasting a flood resulting from a sudden increase in the amount of snowmelt runoff, however, it is necessary to develop a model for an hourly amount or an amount for a shorter interval of snowmelt runoff. In this connection, this chapter will be devoted to estimating the areal distribution of the amount of snowmelt by the heat balance method and to describing a model developed for an hourly amount of snowmelt runoff.

The distribution of the amount of snowmelt in a watershed is usually estimated by the

degree-day (or degree-hour) method, which uses only air temperature and the lapse rate of air temperature (Rango, 1983; Yamada et al., 1985). There are many papers that discuss the amount of ablation of the snowcover obtained by the heat balance method at a given site (Male and Gray, 1981; Male and Granger, 1981; Price and Dunne, 1976; Ishikawa, 1977; Kojima, 1979). In this paper the heat balance method was extended to obtain the areal distribution of the amount of snowmelt. Net radiation, sensible heat flux, and latent heat flux at places in the watershed were calculated by a model using meteorological data obtained at the two stations, one at BH station and the other at WP station on the top of the mountain.

Studying the movement of meltwater in a snowpack is important to the prediction of snowmelt runoff (Wankiewicz, 1978; Colbeck, 1978; Dunne et al., 1976). The movement of meltwater through the snowpack has been simulated by a numerical calculation on the basis of field observations and experimental data (Jordan, 1983a, b). A simple tank model developed by the author for the discharge of meltwater percolated through the snowpack will be explained in this chapter.

Many models for snowmelt runoff have been proposed (Anderson, 1978; Sugawara et al., 1984). A new forecasting model for the hourly amount of snowmelt runoff was devised by improving the runoff tank model; it took into account the percolation of meltwater through the snowpack, as well as the areal distribution of the amount of snowmelt in the watershed estimated by the heat balance method.

IV.2 *Instrumentation*

Two meteorological stations were set up, one at BH station and the other at WP station shown in Fig. 1. The observed periods were from April to May in 1983, 1984, 1985. Air temperature and wind speed were measured in the watershed from time to time. Stream discharge was measured at the outlet of the watershed. The following are the objects observed and recorded continuously at the two stations. a) BH station: Air temperature, wind speed, vapor pressure, surface temperature, global solar radiation, reflected solar radiation, net radiation, and meltwater discharge at the snow-ground interface. b) WP station: Air temperature, wind speed and vapor pressure.

IV.3 *Heat balance equation at snow surface*

The heat balance equation of the snowcover in the snowmelt season is rewritten as,

$$QM = QU = QR + QA + QE - QC + Qr. \tag{3}$$

Each component was explained in Section I.3. In snowmelt seasons, there was little rainfall; so, Qr is ignored. When the meltwater of the surface layer refreezes and the snow temperature falls below 0 °C at night, QC usually becomes negative. The negative QC are compensated for by the positive QC the next morning. In these seasons, QM is zero; QC

can be calculated by QR, QA and QE. Therefore, the amount of energy for snowmelt, QM, can be obtained by QR, QA, and QE. Each component is calculated as follows:

$$QR = SR\downarrow - SR\uparrow + LR\downarrow - LR\uparrow$$
$$= (1-\alpha)SR\downarrow + LR\downarrow - \varepsilon\sigma(T_0+273.2)^4, \quad (17)$$
$$QA = C_a\rho_a C_{pa}(T_1 - T_0)V_1, \quad (18)$$
$$QE = C_e\rho_a L_s(q_1 - q_0)V_1, \quad (19)$$

where $SR\downarrow$ is the global solar radiation, $SR\uparrow$ the reflected solar radiation, $LR\downarrow$ the incoming longwave radiation from the atmosphere, $LR\uparrow$ the outgoing longwave radiation from the surface, α the surface albedo, ε the surface emissivity, σ the Stefan−Boltzmann constant. C_a and C_e are the heat transfer and the mass transfer coefficient, respectively. ρ_a is the air density. C_{pa} is the specific heat of air. L_s is the quantity of heat of sublimation. T_1, q_1, and V_1 the air temperature, specific humidity and wind speed at the height of 1 m above the snow surface, respectively. T_0 is the surface temperature, and q_0 the specific humidity at the snow surface. The heat transfer coefficient was determined by field observations under stable conditions: $C_a = 2.2\times10^{-3}$ (Ishikawa et al., 1982). The value of C_e is assumed to be equal to the value of C_a under stable conditions (Male and Granger, 1981).

IV. 4 *Calculating method for heat balance in watershed*

The watershed was divided by a 125 m × 125 m mesh. The amount of energy for the snowmelt at each point of the grid was calculated as follows:

1) Air temperature, wind speed and specific humidity in the watershed

The areal distributions of air temperature, wind speed and specific humidity were assumed to be a function of altitude. Based on the distributions of air temperature observed and minimum air temperature observed in the watershed, the following results were obtained: (a) In the upper region, above the altitude of 400 m a.s.l., the lapse rate of air temperature was 0.6×10^{-2} °Cm^{-1}. (b) In the lower region, the wind speed was generally slow and radiative cooling occurred strongly on a clear night, and the height of the inversion layer reached only 400 m a.s.l. Then the air temperature at altitude $T_1(h)$ was obtained by using the observed air temperatures at the two stations as follows:

For $h \geq 400$ m,

$$T_1(h) = T_1(\mathrm{WP}) + \Gamma(580 - h) \quad [^\circ\mathrm{C}], \quad (20a)$$

for $h < 400$ m,

$$T_1(h) = T_1(400) + ((T_1(\mathrm{BH}) - T_1(400))/(400-285))(h-400) \quad [^\circ\mathrm{C}],$$
$$T_1(400) = T_1(\mathrm{WP}) + \Gamma(580-400) \quad [^\circ\mathrm{C}], \quad (20b)$$

where h is the altitude (m a.s.l.), T_l(WP) is the air temperature at WP station, T_l(BH) is the air temperature at BH station. For the value of Γ, 0.6×10^{-2} °Cm^{-1} is used.

The wind speed and specific humidity were assumed to vary linearly with the altitude. Lapse rates can be calculated from the observed data at the two stations; and the wind speed and specific humidity at the altitude of h were obtained as follows:

$$V_l(h)=((V_l(\mathrm{WP})-V_l(\mathrm{BH}))/(580-285))(h-285)+V_l(\mathrm{BH})\ [\mathrm{m/s}], \tag{21}$$
$$q_l(h)=((q_l(\mathrm{WP})-q_l(\mathrm{BH}))/(580-285))(h-285)+q_l(\mathrm{BH})\ [\mathrm{Pa/Pa}]. \tag{22}$$

2) Net radiation

Net radiation, QR, can be calculated by Equation (16), where α and $LR\downarrow$ are assumed to be constant at any place in the watershed. The values of α and $LR\downarrow$ can be obtained by the meteorological data observed at BH station as follows:

$$\alpha=SR\uparrow/SR\downarrow \tag{23}$$
$$LR\downarrow=QR-(1-\alpha)\mathrm{SR}\downarrow+\varepsilon\sigma(T_0+273.2)^4. \tag{24}$$

Global solar radiation, $SR\downarrow$, consists of direct solar radiation, Sb, and diffuse solar radiation, Sd, as follows:

$$SR\downarrow=Sb+Sd. \tag{25}$$

2.1) Direct solar radiation

The direct solar radiation at point j, $(Sb)_j$, can be calculated as follows from the direct solar radiation at BH station, $(Sb)_{\mathrm{BH}}$, and the ratio of the calculated direct solar radiation at point j, $(Sb)_{j.\mathrm{cal}}$, to the calculated one at the BH station, $(Sb)_{\mathrm{BH.cal}}$:

$$(Sb)_j=((Sb)_{j.\mathrm{cal}}/(Sb)_{\mathrm{BH.cal}})(Sb)_{\mathrm{BH}}. \tag{26}$$

The calculated direct solar radiation on the slope varies with the slope angle, the direction of the slope and the screen effect of a ray path. The theoretical direct solar radiation $(Sb)_{\mathrm{cal}}$ is given by (Barry, 1981),

$$(Sb)_{\mathrm{cal}}=SB(Y1+Y2), \tag{27a}$$
$$Y1=CZ\cos(SL), \tag{27b}$$
$$Y2=\sin(SL)((\cos(AS)((CZ\sin(PH)-\sin(DE))/\cos(PH))) +(\sin(AS)\cos(DE)\sin(WT))), \tag{27c}$$
$$CZ=\sin(PH)\sin(DE)+\cos(PH)\cos(DE)\cos(WT), \tag{27d}$$

where PH is the latitude, DE the declination angle of the sun (north positive), WT the hour angle of the sun from the apparent noon (clockwise positive), SL the slope angle, AS the azimuth of the slope, and SB the solar constant. Moreover, the effect of screening is considered; namely, when the direct solar beam is intercepted by obstacles of the terrain, $(Sb)_{\mathrm{cal}}=0$.

2.2) Diffuse solar radiation

Diffuse solar radiation at point j, $(Sd)_j$, can be calculated as,

$$(Sd)_j=(Sd)_{BH}\cos^2(SL/2), \tag{28}$$

where $(Sd)_{BH}$ is the diffuse solar radiation at BH station and SL is the slope angle (Barry, 1981).

2.3) Net radiation

The outgoing longwave radiation from the snow surface, $LR\uparrow$, is calculated by the following equation by regarding the snow surface as nearly a black body and using 0.99 as the surface emissivity ε of it:

$$LR\uparrow=\varepsilon\sigma(T_0+273.2)^4. \tag{29}$$

The surface temperature T_0 is estimated by an empirical formula using the air temperature T_1 during the snowmelting season obtained at BH station (Fig. 30).

$$T_0=0.81T_1-3.0 \quad [°C] \quad \text{for } T_1\leq 3.7°C, \tag{30a}$$
$$T_0=0.0 \quad [°C] \quad \text{for } T_1>3.7°C. \tag{30b}$$

Net radiation at point j is, therefore, given by,

$$\begin{aligned}(QR)_j=&(1-\alpha)(((Sb)_{j.cal}/(Sb)_{BH.cal})(Sb)_{BH}+(Sd)_j)\\&+((QR)_{BH}-(1-\alpha)(SR\downarrow)_{BH}+\varepsilon\sigma((T_0)_{BH}+273.2)^4)\\&-\varepsilon\sigma((T_0)_j+273.2)^4.\end{aligned} \tag{31}$$

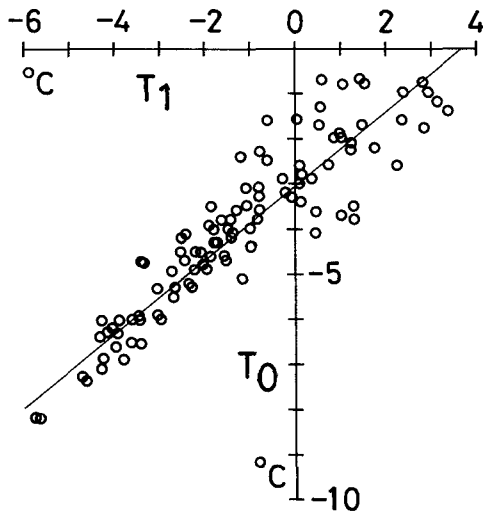

Fig. 30 Relation between the mean hourly air temperature, T_1, and the surface temperature of the snowcover, T_0, for the snowmelt season in April 1984 at BH station.

Table 7 Global solar radiation in the watershed, *MJ*, calculated by changing the ratio of diffused solar radiation to global solar radiation at BH station in the period, April 13-30, 1984. The areal ratio is also shown in the right column.

altitude (m)	ratio of diffused solar radiation			areal ratio
	0.0	0.5	1.0	
280-300	111	111	112	0.06
300-350	108	109	110	0.12
350-400	107	108	109	0.15
400-450	106	107	108	0.19
450-500	110	110	110	0.26
500-550	105	106	108	0.17
550-600	110	110	111	0.06
600-630	97	104	111	0.01
280-630	110	111	111	1.00

There is no data to separate the direct solar radiation, Sb, and diffuse solar radiation, Sd, from the global solar radiation, $SR\downarrow$. Table 7 shows an experiment to examine the effect of the ratio of Sd to $SR\downarrow$ on the global solar radiation. When the ratio of Sd to $(SR\downarrow)_{BH}$ changed from 0 to 1, the calculated $(SR\downarrow)_{cal}$ varied within 1 %. Therefore, the global solar radiation was calculated as the direct solar radiation.

3) Sensible heat flux

The values of T_1, V_1, and T_0 were obtained at all grid points for calculating QA by Equation (18).

4) Latent heat flux

The specific humidity at the snow surface, q_0, was assumed to be the saturated vapor pressure of ice at T_0 for calculating QE by Equation (19).

IV. 5 *Results of meteorological observations*

Variations in air temperature and wind speed at the two stations in 1983 and 1984 are shown in Fig. 31 (solid line: at BH station, broken line: at WP station). In the lower region, the wind speed is generally slow, strong radiative cooling occurs at night, and air temperature often falls below 0 °C. On the other hand, in the upper region, the wind speed is fast almost all day long, radiative cooling is weak, and air temperature seldom falls below 0 °C.

IV. 6 *Characteristics of energy for snowmelt in watershed*

The amount of energy for snowmelt can be calculated by an areal heat balance model. Variations in areal mean heat balance components in an altitudinal range from 280 − 300 m

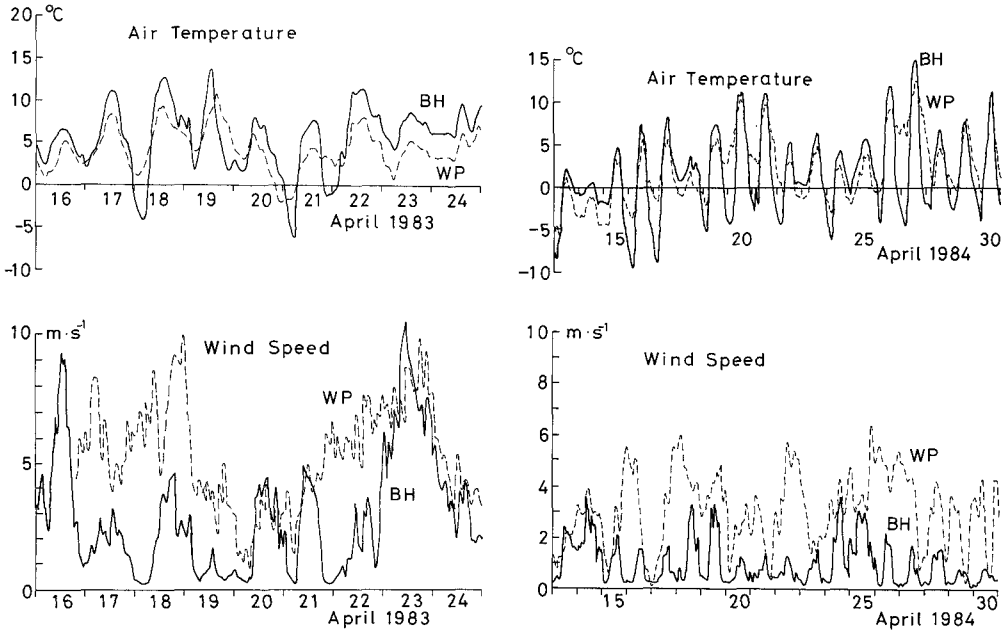

Fig. 31 Variations in air temperature and wind speed in 1983 and 1984. Solid line: at BH station; broken line: at WP station.

a.s.l. and 550 − 600 m a.s.l. are shown in Fig. 32. The solid line, broken line, and dotted line represent net radiation, sensible heat flux, and latent heat flux, respectively. Net radiation reached the daily maxima of 1.0 − 1.5 $MJm^{-2}h^{-1}$ around noon and decreased to the daily minima of −0.3 − −0.4 $MJm^{-2}h^{-1}$ at night. The sensible heat flux reached the daily maxima of about 0.5 $MJm^{-2}h^{-1}$ at 1300 − 1400 LST and fell to nearly 0 $MJm^{-2}h^{-1}$ at night. As for the latent heat flux, evaporation occurred in the daytime and slight condensation at night.

Net radiation was nearly the same everywhere in the daytime, but at nighttime, when strong radiative cooling occurred, it had a slightly larger negative value in the upper region than that in the lower region. This difference is due to the higher snow surface temperature in the upper region, and the outgoing longwave radiation which was larger in the upper region than in the lower region (see Equation (29)). The amplitudes of diurnal fluctuations in sensible and latent heat fluxes were larger in the upper region than those in the lower region, since the wind speed was relatively fast almost all the time and the air temperature was seldom fell below 0 °C in the upper region.

The heat balance components integrated for the period from April 13 to April 30, 1984, are shown in Fig. 33. The calculated amount of energy for snowmelt, QM, in the upper region was 1.2 − 1.3 times that in the lower region. The sensible heat flux, QA, and the

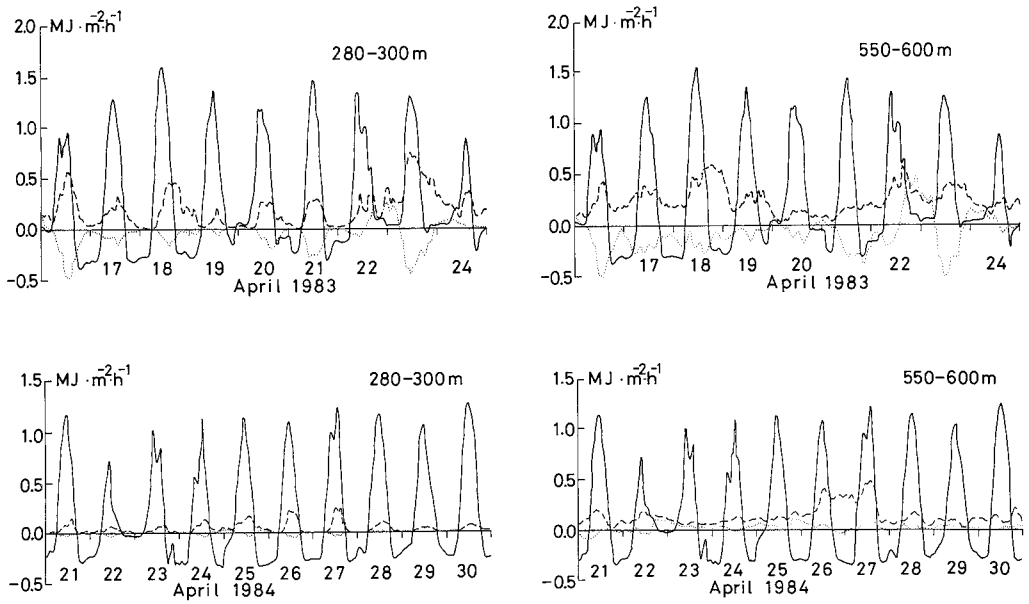

Fig. 32 Areal mean heat balance components between 280–300, 550–600 m a.s.l. in 1983 and 1984.
Solid line: net radiation, broken line: sensible heat flux, dotted line: latent heat flux.

latent heat flux, QE, were also larger in the upper region, whereas the net radiation, QR, was almost the same everywhere. As seen in Fig. 34, the ratio of net radiation to the amount of energy for snowmelt, QR/QM, is 0.8 in the lower region, and decreases to 0.5 in the upper region, whereas the ratio of the sensible heat flux to the amount of energy for snowmelt, QA/QM, is 0.2 in the lower region, and increases to 0.4 in the upper region.

IV.7 *Method for calculating hourly snowmelt runoff*

A runoff model was developed for snowmelt season. The snowmelting rates in the watershed were calculated by the areal heat balance method described in Section IV. 4. The snowmelt from the snow surface moves through the snowpack and ground, and then runs off as stream flow. The runoff process can be divided into two parts, the meltwater movement through the snowpack, and its movement under the ground toward the stream.

IV.7.1 *Discharge of meltwater percolated through snowpack*

The discharge of meltwater at the snow-ground interface was measured using a shallow lysimeter, which was buried in the ground (Fig. 3). The rate of surface snowmelt calculated by the heat balance method (dotted line) and the discharge at the snow-ground interface (solid line) are shown in Fig. 35. In this observation, the snow depth decreased from about

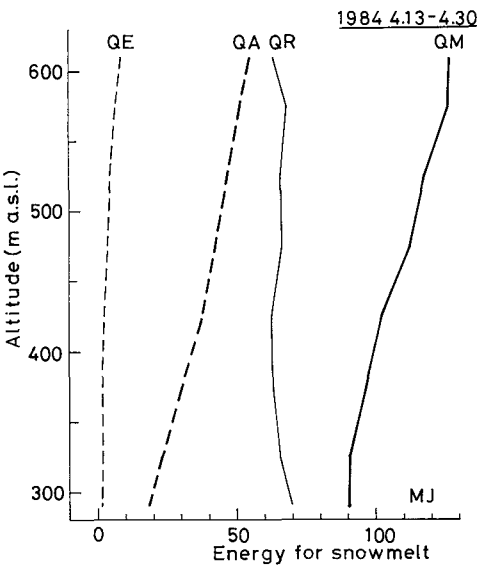

Fig. 33 Altitudinal distribution of integrated heat balance components, integrated for the period from April 13 to 30 in 1984.
Thick solid line: amount of energy for snowmelt, *QM*.
Thin solid line: net radiation, *QR*.
Thick broken line: sensible heat flux, *QA*.
Thin broken line: latent heat flux, *QE*.

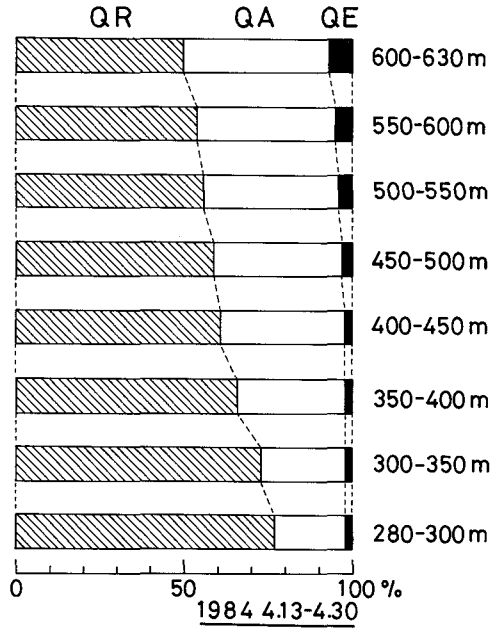

Fig. 34 The ratio of the heat balance components (*QR*, *QA*, and *QE*) to the amount of energy for snowmelt, *QM*, at various altitudes averaged for April 13–30, 1984.

0.8 m to 0.5 m. The peak of the snowmelt amount at the snow surface was attenuated, delaying about 3 to 4 hours in the discharge at the bottom of the snowcover (Kojima and Motoyama, 1984).

A "tank model" was devised to calculate the discharge from the snowpack (Sugawara et al., 1984). In the tank model, the estimated amount of surface meltwater, M, by the heat balance method is supplied to the tank every hour and the calculated amount of runoff at the snow-ground interface, r_b, is discharged from the outlet of the tank (Fig. 36), i.e.,

$$r_b(i)=0.1D(i)+0.25(D(i)-9.0)\ [\mathrm{mmh^{-1}}] \quad \text{for } D(i)\geq 9.0 \text{ mm},$$
$$r_b(i)=0.1D(i)\ [\mathrm{mmh^{-1}}] \quad \text{for } D(i)<9.0 \text{ mm}, \tag{32a}$$
$$D(i+1)=D(i)+M(i+1)-r_b(i)\ [\mathrm{mm}], \tag{32b}$$

where i is the time step and D is the height of storage in the tank. The parameter of the tank structure was determined by referring to the recession rates in a hydrograph at the snow-ground interface (Fig. 37). The simulated discharge of meltwater from the snowpack is

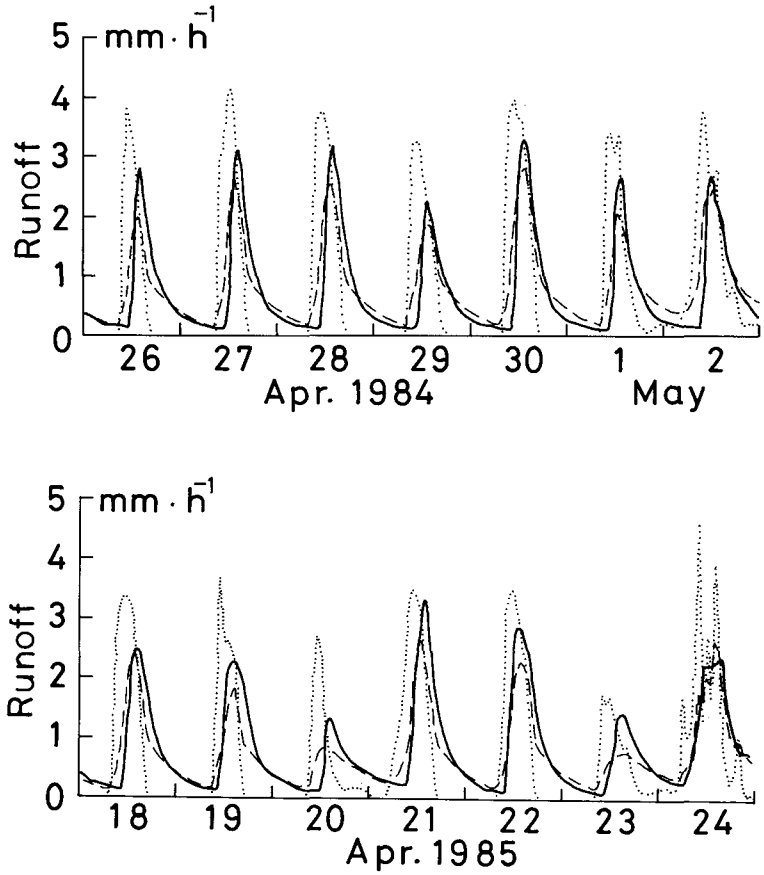

Fig. 35 Hourly amount of snowmelt at the snow surface estimated by heat balance (dotted line), observed amount of melt water collected by the lysimeter at the bottom of the snowpack (solid line) and calculated amount of meltwater by the tank model (broken line) in 1984 and 1985. Snow depth varied from 0.8 m on April 26 to 0.5 m on May 2, 1984 and from 0.7 m on April 18 to 0.45 m on April 24, 1985.

shown in Fig. 35 by a broken line. The observed and simulated discharges from the snowpack agree well.

The recession rates of the recession curve in the hydrograph at the snow-ground interface were 0.1 h^{-1} for discharges smaller than 0.5 mmh^{-1} and 0.25 h^{-1} for discharges larger than 0.5 mmh^{-1}. This suggests that the flow process of the meltwater through the snowpack changes, dependent on the meltwater flux.

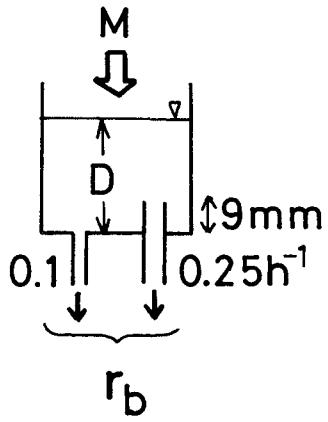

Fig. 36 Derived tank model for movement of meltwater through the snowpack.

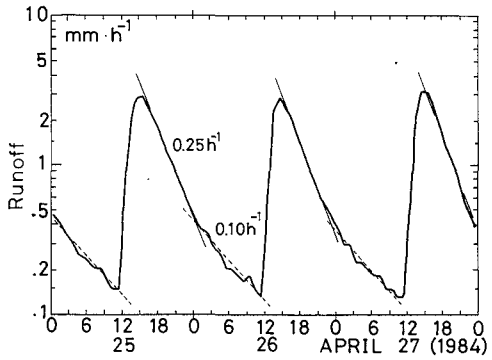

Fig. 37 Hydrograph of discharge at the snow-ground interface.

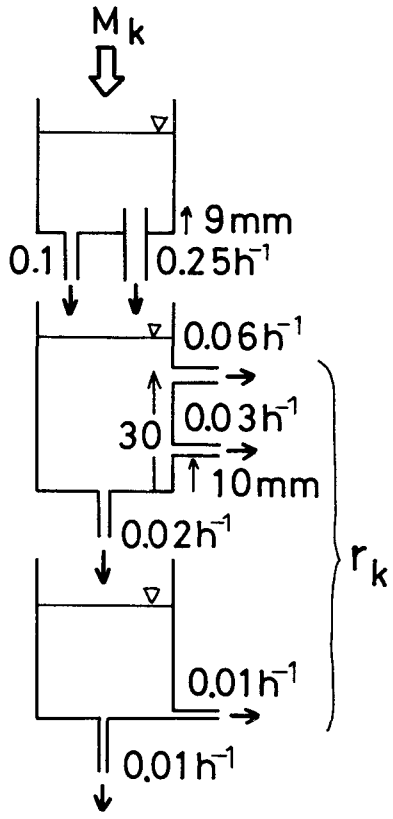

Fig. 38 Derived tank model calculating the hourly amount of runoff. The coefficients of tank's outlet are shown in the unit of h^{-1}. The heights of the outlet are shown in the unit of mm.

IV.7.2 *Determination of the runoff model*

The watershed was divided into eight sub-watersheds. Each sub-watershed represents an interval of 50 m in altitude. Hourly amount of snowmelt for each sub-watershed was calculated by the areal heat balance method. The same runoff tank model was developed for each sub-watershed. A series of three tanks of the storage type was used (Fig. 38). The upper tank was of the same model as the one which simulated the runoff rate from the snowpack. The structures of the other tanks were determined by the recession rates at various discharges in the runoff hydrograph (Fig. 39). The speed of channel flow from the sub-watershed to the outlet of the entire watershed was assumed to be 0.5 kmh^{-1} (Kobayashi

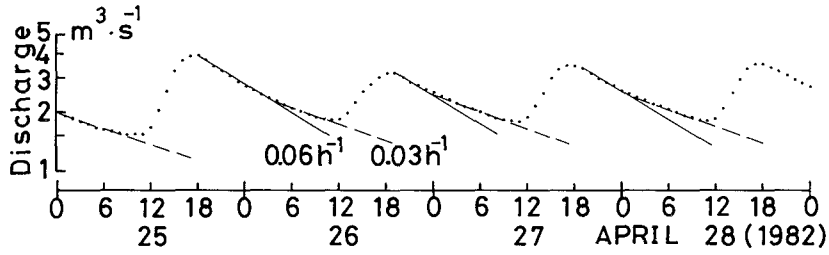

Fig. 39 Runoff hydrograph for the period from 25 April to 28 April in 1982.

and Uematsu, 1977). The sum of the runoff from all the sub-watersheds, $r(t)$, was obtained as the total discharge from the entire watershed, $Q(t)$, i.e.,

$$Q(t)=\sum_{k=1}^{8} r_k(t-0.5d_k)A_k, \tag{33}$$

where d_k is the mean distance from the k-th sub-watershed to the outlet of the main watershed (unit of km) and A_k the drainage area of the k-th sub-watershed.

IV.7.3 *Results*

The observed and calculated hydrographs for 1983 and 1984 are plotted in Fig. 40 by solid and broken lines, respectively. The hourly amount of snowmelt runoff was estimated well by the runoff model. The timing and the amount of peak discharge matched especially well for the discharge from 2 to 8 m^3s^{-1}.

On April 22−23, 1983, it rained and a snowmelt flood occurred. This flood was also simulated, indicating that the above method for calculating snowmelt runoff is useful for forecasting the snowmelt flood.

This model was applied which was used to calculate the discharge of meltwater percolated through the snowpack to the upper tank structure. The discharge at the bottom of the snowcover was dependent upon by the structure of the snowpack and the snow depth. Therefore, the flux of meltwater varied gradually as it passes through the snowpack. The height of the tank's outlet should be changed according to the structure of the snowpack and the snow depth (Sugawara et al., 1984). The varying thickness of the snowcover has been shown to affect alpine stream flow (Woo and Slaymaker, 1975). The spatial distributions of snow depth in the watershed were examined in the period. Since the height of snow depth was only about 1.5 − 0.5 m, the height of the outlet of the upper tank was fixed. When the snowpack disappeared, the upper tank was eliminated for runoff analysis.

IV.8 *Conclusion*

The distributions of the amount of snowmelt in the watershed were estimated by the heat balance method on the basis of the observed meteorological data at two stations. The hourly hydrograph was simulated using the calculated amount of snowmelt. The following

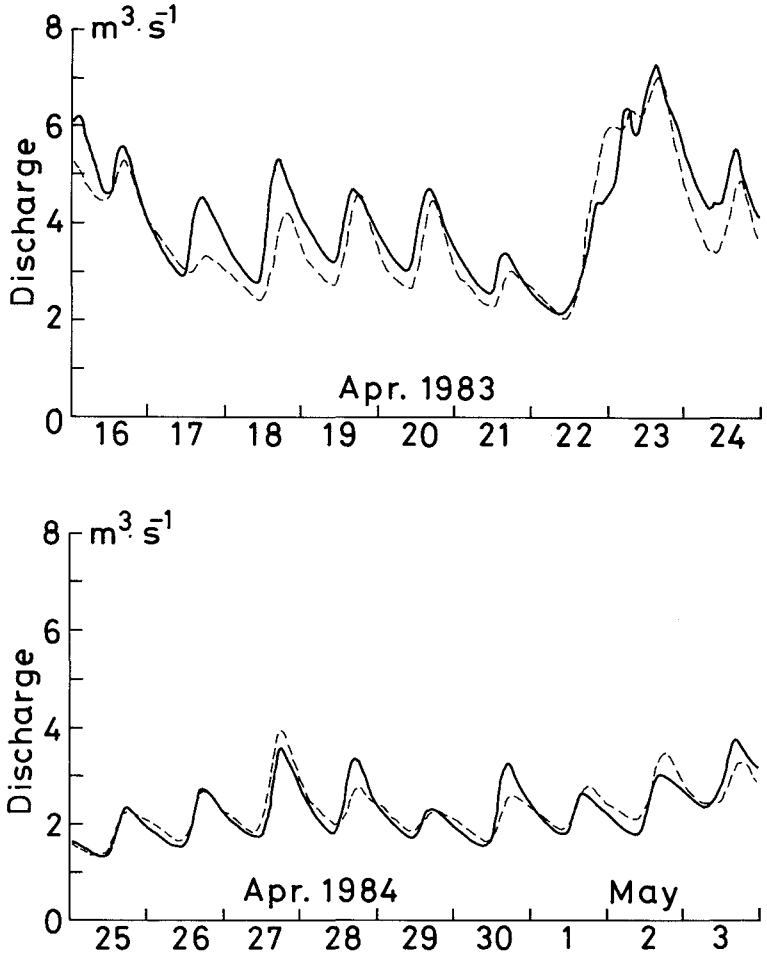

Fig. 40 Hydrographs in 1983 and 1984.
Solid line: observed stream discharge, broken line: calculated stream discharge.

results were obtained:

1. The distribution of the hourly amount of snowmelt in the watershed was estimated by the areal heat balance method. Net radiation, sensible heat flux, and latent heat flux were calculated at any given place in the watershed.

2. The total amount of snowmelt calculated in the upper region was 1.2 – 1.3 times that in the lower region during April 13 – 30, 1984. Net radiation was almost the same everywhere, but the sensible and latent heat fluxes were larger in the upper region.

3. A tank model with two outlets simulated well the discharge of meltwater percolated through the snowpack.

4. The hourly amount of snowmelt runoff was successfully simulated by the tank model for two seasons using the calculated areal distribution of the amount of snowmelt by the heat balance method. The runoff tank model was composed of three tanks. The upper tank specifically represented the discharge of meltwater through the snowpack.

V. Concluding remarks

The amount of snowmelt runoff was studied during the winter and the snowmelt season. The following results were obtained :

1. Based on the observed amount of bottom-melt at the outlet, the amount of bottom-melt at the watershed was estimated using the areal distributions of air temperature and snow depth.

2. The amount of snowmelt at the snow-ground interface (bottom-melt) supplied about one half of the runoff water to the watershed. It was found that the bottom-melt plays an important role in the water balance during the winter.

3. Based on the hydrological observations, 90 percent of the snowcover in the watershed ran off as stream flow during the snowmelt season.

4. The distribution of hourly amount of snowmelt in the watershed was estimated by the areal heat balance method, in which net radiation, sensible heat flux, and latent heat flux were calculated at all place in the watershed.

5. The discharge of meltwater percolated through the snowpack was simulated by a simple tank model.

6. Forecasting methods of the hourly or daily amount of snowmelt runoff using the advanced tank model were developed for both winter and snowmelt seasons.

In future studies, these methods should be applied to other watersheds so that the general rule will be found to explain the runoff process in snow-covered and snow-free watersheds.

Acknowledgments

The author is grateful to the staff members of the Uryu Experimental Forest of Hokkaido University for their help in this study. And for helpful advice and useful suggestions, he also wishes to thank Drs. Y. Kodama, T. Yamada, R. Naruse, E. Akitaya, N. Ishikawa, D. Kobayashi, of Institute of Low Temperature Science ; Prof. K. Nakao of Faculty of Science, Hokkaido University ; and Mr. H. Aburakawa of Hokkaido University of Education ; and for continuous discussions and encouragement to Profs. S. Kinosita and K. Kojima.

Notation

A	total watershed area [11.2 km^2]
$A(h)$	altitudinal distribution of sub-watershed area in Fig. 21
AS	azimuth of slope
A_s	remaining area of snowcover [km^2]
C_a	heat transfer coefficient
C_e	mass transfer coefficient
C_{pa}	specific heat of air [Jkg^{-1}K^{-1}]
C_{ps}	specific heat of snow [Jkg^{-1}K^{-1}]
CZ	variable
B	constant in Fig. 10
D	height of storage in tank [mm]
DA	height of storage in upper tank [mm]
DB	height of storage in lower tank [mm]
DE	declination angle of sun (north positive)
E	amount of mass transfer at snow surface [mmd^{-1}]
ET	amount of evapotranspiration [mmd^{-1}]
F	constant in Fig. 10
HS	snow depth [cm or m]
HW	snow water equivalent [10kgm^{-2} or cm-water]
h	altitude [m a.s.l.]
i	time step [hours or days]
I	integrated precipitation in addition to areal mean snow water equivalent [cm-water]
j	number of point in serial order
k	number of sub-watershed in serial order
L_m	quantity of heat for melting ice [Jkg^{-3}]
L_s	quantity of sublimation heat [Jkg^{-3}]
$LR\downarrow$	incoming longwave radiation from atmosphere [kWm^{-2}]
$LR\uparrow$	outgoing longwave radiation from surface [kWm^{-2}]
M	amount of snowmelt [mmd^{-1}]
M_b	calculated amount of bottom-melt in watershed [mmd^{-1}]
m_b	amount of bottom-melt [mmd^{-1}]
m_b(HF)	calculated amount of bottom-melt by heat balance method [mmd^{-1}]
m_b(LY)	observed amount of bottom-melt by lysimeter [mmd^{-1}]
O	integrated runoff depth [cm-water]
P	precipitation [mmd^{-1}]

PH	latitude
q_1	specific humidity at height of 1 m above snow surface [Pa/Pa]
q_0	specific humidity at snow surface [Pa/Pa]
Q	amount of snowmelt runoff in Fig. 22 [cm-water]
$Q(t)$	amount of snowmelt runoff [m^3s^{-1}]
Q'	amount of runoff in Fig. 22 [cm-water]
QA	sensible heat flux from air [kWm^{-2}]
QB	flux of heat at snow-ground interface [kWm^{-2}]
Q_{cg}	conductive heat flux in ground [kWm^{-2}]
Q_{cs}	conductive heat flux in snow near snow-ground interface [kWm^{-2}]
QC	conductive heat flux through snowcover near snow surface [kWm^{-2}]
QE	latent heat flux [kWm^{-2}]
QR	net radiation [kWm^{-2}]
Qr	flux of heat from rain [kWm^{-2}]
QM	amount of energy for snowmelt [kWm^{-2}]
QU	flux of heat at snow-air interface [kWm^{-2}]
r	runoff depth [mmd^{-1}]
r_b	discharge of meltwater from snow-ground interface [mmh^{-1}]
r_{cal}	calculated daily amount of runoff depth [mmd^{-1}]
r_{obs}	observed daily amount of runoff depth [mmd^{-1}]
R	amount of rainfall [mmd^{-1}]
Sb	direct solar radiation [kWm^{-2}]
Sd	diffuse solar radiation [kWm^{-2}]
S_d	groundwater storage [mm]
SB	solar constant
SL	slope angle
$SR\downarrow$	global solar radiation [kWm^{-2}]
$SR\uparrow$	reflected solar radiation [kWm^{-2}]
$S1$	amount of runoff in Fig. 22 [cm-water]
$S2$	amount of runoff in Fig. 22 [cm-water]
T_o	surface temperature of snowcover [°C]
T_a	air temperature [°C]
T_1	air temperature at height of 1 m above snow surface [°C]
V_1	wind speed at height of 1 m above snow surface [m/s]
WT	hour angle of sun from apparent noon (clockwise positive)
$Y1$	variable
$Y2$	variable
z	height above bottom of snowcover [cm]
z'	normalized height above bottom of snowcover

α	surface albedo
ρ_a	air density $[10^3 kgm^{-3}]$
ρ_s	snow density $[10^3 kgm^{-3}]$
ε	surface emissivity
σ	Stefan-Boltzmann constant $[5.67 \times 10^{-8} Wm^{-2}K^{-4}]$

References

Aburakawa, H. 1980 Snow survey by snow depth recorder in Teshio mountainous region. *Low Temp. Sci., Ser.* **A**, **39**, 63−74 (in Japanese with English summary).

Anderson, E. A. 1978 Streamflow simulation models for use on snow covered watersheds. Proc. of modeling of snow cover runoff, (S. C. Colbeck and M. Ray eds.), U.S. Army Cold Regions Research and Engineering Laboratory, Hanover, New Hampshire, 26−28 September 1978, 336−350.

Arai, T. 1976 Nippon no mizusyushi -Gaiyo to mondaiten- [Water balance in Japan -Outlines and problems-]. Rissyo Daigaku Bungakuburonshu, 56, 95−125 (in Japanese).

Arai, T. 1980 Nippon no mizu [Water balance in Japan]. Sanseido, 278pp (in Japanese).

Barry, R. G. 1981 Mountain weather and climate. Methuem, London and New York, 313pp.

Colbeck, S. C. 1978 The physical aspects of water flow through snow. *Advances in Hydroscience*, **11**, 165−206.

Dunne, T., Price, A. G. and S. C. Colbeck 1976 The generation of runoff from subarctic snowpack. *Water Resour. Res.*, **12**, 677−685.

Ishikawa, N. 1977 Studies of radiative cooling at land basins in snowy season. Contr. Inst. Low Temp. Sci., **A**, **27**, 46pp.

Ishikawa, N., S. Kobayashi and K. Kojima 1982 Measurement of sensible heat flux in the snow-melting season I. *Low Temp. Sci., Ser.* **A**, **41**, 109−116 (in Japanese with English Summary).

Ishikawa, N., K. Kojima, H. Motoyama and Y. Yamada 1984 Radiation measurements of snowy season in 1983−84 at Sapporo. *Low Temp. Sci., Ser.* **A**, **43**, Data Report, 51−58 (in Japanese).

Ishikawa, N., K. Kojima and H. Motoyama 1985 Radiation measurements of snowy season in 1983−84 at Sapporo. *Low Temp. Sci., Ser.* **A**, **44**, Data Report, 40−45 (in Japanese).

Izumi, K. and T. Huzioka 1975 Studies of metamorphism and thermal conductivity of snow. *Low Temp. Sci., Ser.* **A**, **33**, 91−102 (in Japanese with English summary).

Jordan, P. 1983 Meltwater movement in a deep snowpack, 1. Field observations. *Water Resour. Res.*, **19**(4), 971−978.

Jordan, P. 1983 Meltwater movement in a deep snowpack, 2. Simulation model. *Water Resour. Res.*, **19**(4), 979−985.

Kobayashi, D. and T. Uematsu 1977 Stream temperature during snowmelt period III. *Low Temp. Sci., Ser.* **A**, **35**, 167−178 (in Japanese with English summary).

Kojima, K. 1957 Viscous compression of natural snow layer III. *Low Temp. Sci., Ser.* **A**, **16**, 167−196 (in Japanese with English résumé).

Kojima, K. 1967 Densification of seasonal snow cover. In Physics of Snow and Ice, Part 1 (H. Ōura *ed.*), Inst. Low Temp. Sci., Sapporo, 929−952.

Kojima, K., D. Kobayashi, S. Kobayashi, H. Aburakawa and N. Ishikawa 1970 Studies of snow melt, runoff, and heat balance in a small drainage area in Moshiri, Hokkaido I. *Low*

Temp. Sci., Ser. **A**, **28**, 175−190 (in Japanese with English summary).
Kojima, K., D. Kobayashi, H. Aburakawa, R. Naruse, K. Ishimoto, N. Ishikawa and S. Takahashi 1971 Studies of snow melt, runoff, and heat balance in a small drainage area in Moshiri, Hokkaido II. *Low Temp. Sci., Ser.* **A**, **29**, 159−176 (in Japanese with English summary).
Kojima, K., H. Motoyama and Y. Yamada 1983 Estimation of melting rate of snow by simple formulae using only air temperature. *Low Temp. Sci., Ser.* **A**, **42**, 101−110 (in Japanese with English summary).
Kojima, K. and H. Motoyama 1984 Time lag of meltwater percolation through a snow cover. *Low Temp. Sci., Ser.* **A**, **43**, 181−184 (in Japanese).
Kojima, K. and H. Motoyama 1985 Melting and heat exchange at the bottom of a snow cover. *Annals of Glaciol.*, **6**, 276−277.
Leaf, C. F. 1971 Areal snow cover and disposition of snowmelt runoff in central Colorado. USDA For. Serv. Res. Pap. RM−66, Rocky Mt. For. and Range Exp. Sta., Fort Collins, Colo., 19pp.
Male, D. H. and R. J. Granger 1981 Snow surface energy exchange. *Water Resour. Res.*, **17**, 609−627.
Male, D. H. and D. M. Gray 1981 Chp. 9. Snowcover ablation and runoff in Handbook of Snow. Principles, Processes, Management and Ice. Pergamon Press, Tronto, 360−436.
Motoyama, H., D. Kobayashi and K. Kojima 1983a Water balance at a small watershed during the snowmelt season I. *Low Temp. Sci., Ser.* **A**, **42**, 123−133 (in Japanese with English summary).
Motoyama, H., D. Kobayashi and K. Kojima 1983b Water balance at a small watershed during the snowmelt season II -Runoff analysis-. *Low Temp. Sci., Ser.* **A**, **42**, 135−146 (in Japanese with English summary).
Motoyama, H. and K. Kojima 1985 Estimation model for the depth of a dry snow cover -Based on the viscous compression theory of seasonal snow cover-. *Low Temp. Sci., Ser.* **A**, **44**, 15−25 (in Japanese with English summary).
Motoyama, H., D. Kobayashi and K. Kojima 1986 Effect of melting at the snow-ground interface on the runoff during winter. *Jpn. J. Limnol.*, **47**(2), 163−174.
Motoyama, H., D. Kobayashi and K. Kojima 1986 Water balance and runoff analysis at a small watershed during the snowmelting season. Cold Region Hydrology Symposium, American Water Resources Association, 297−304.
Ono, S and R. Kawaguchi 1974 Syoryuiki ni okeru choseturyo suitei to 'sinrin no eikyo' no kaiseki [Studies of estimation of snowcover and effect of forest on snow at small watersheds]. Ringyo Sikenjo Tohoku Sijo. Nenpou, 114−119 (in Japanese).
Price, A. G. and T. Dunne 1976 Energy balance computations of snowmelt in a subarctic area. *Water Resour. Res.*, **12**, 686−694.
Rango, A. 1983 Application of a simple snowmelt-runoff model to large river basins. 51st Annual Meeting Western Snow Conference, Vancouver, Washington, 89−99.
Sugawara, M., Watanabe, E. Ozaka and Y. Katsuyama 1984 Tank model with snow component. Research Notes of the National Research Center for Disaster Prevention, 65, 1−293.
Wankiewics, A. 1978 A review of water movement in snow. Proc. modeling of snow cover runoff, (S. C. Colbeck and M. Ray eds.), U. S. Army Cold Regions Research and Engineering Laboratory, Hanover, New Hampshire, 26−28 September 1978, 222−252.
Warren, S. G. 1982 Optical properties of snow. Reviews of Geophysics and Space Physics, 20, 67−89.
Woo, M. K. and O. Slaymaker 1975 Alpine stream flow response to variable snowpack thickness and extent. *Geografiska Annaler*, **3**−**4**, 201−212.

Yamada, T., H. Motoyama and K. B. Thapa 1985 Mass balance study of a glacier system from hydrological observations in Langtang Valley, Nepal Himalaya. *Annals of Glaciol.*, **6**, 318–320.